ELECTROCHEMICAL BEHAVIOUR OF SOME ORGANOMETALLIC COMPOUNDS CONTAINING IRON AND MOLYBDENUM

by

Keith L. Daries
B.Sc.(Hons)

A thesis submitted in the fulfilment of the requirements for the Degree of Master of Science in the Department of Chemistry, University of Cap[e Town, under the supervision of Professors J. R. Moss (UCT) and A. M. Crouch (UWC).

November 1995

CONTENTS

Chapter 2

Results and discussion

Chapter 3

Acknowledgments

I would like express my sincere thanks to the following persons:

My supervisors, especially Prof. Moss for his encouragement during the writing up of this manuscript;

Robyn George for synthesising some of the compounds;

Dr. Selwyn Mapolie for proof reading this manuscript and his helpful discussions;

My late parents.

Abstract

The electrochemical behaviour of some mononuclear alkyl compounds of the types $CpFe(CO)_2(CH_2)_nCH_3$ (n = 0 to 11, Cp = η-C_5H_5), $CpMo(CO)_3(CH_2)_nCH_3$ (n = 3,4,17) have been investigated in aprotic solvents. The cyclic voltammograms obtained for all the iron alkyl compounds suggest similar behaviour after the initial oxidation. The oxidation potentials showed no linear correlation with the corresponding lengths of the alkyl chain, but could, however, be interpreted with the available Tolman's χ-values. The subsequent CO insertion reaction to give an acyl species was found to be dependent on the nucleophilicity of the solvent.

The relative rates of decarbonylation of the acyl species could be assessed through cyclic voltammetry.

The electrochemical behaviour of heterobimetallic complexes of the type $CpFe(CO)_2(CH_2)_nMo(CO)_3Cp$ (n = 3 to 6) was found to be solvent dependent. The anodic waves obtained for these complexes in acetonitrile showed up as two closely spaced waves. Our results suggest that the two metals in $CpFe(CO)_2(CH_2)_nMo(CO)_3Cp$ behave independently, with the iron end of the molecule being oxidized first, followed by CO insertion/alkyl migration at this end.

Parts of this thesis have been presented as posters at the following conferences:

Daries, K., Moss, J.R., Crouch, A.M. "The electrochemical behaviour of bridged metal complexes of Fe and Mo in non-aqueous media." 31st Convention of the South African Chemical Institute, June 1991, Grahamstown, South Africa.

Daries, K.L., Moss, J.R., Crouch, A.M. "Non-aqueous voltammetry of heterobimetallic compounds of iron and molybdenum." Inorganic '92, SACI, June 1992, Warmbad, South Africa.

Daries, K.L., Moss, J.R., Crouch, A.M. "Non-aqueous voltammetry of $CpFe(CO)_2R$ and $CpMo(CO)_3R$, where R = alkyl chain of varying chain length." 32nd Convention of the South African Chemical Institute, January 1993, Midrand, South Africa.

ABBREVIATIONS

The following abbreviations are used in this thesis:

Cp	η^5-C_5H_5
Cp′	η^5-$C_5H_4CH_3$
Cp*	η^5-$C_5(CH_3)_5$
Me	methyl group
Ph	phenyl group
CV	Cyclic voltammogram
CAN	cerium ammonium nitrate
Bz	benzyl group
$TBABF_4$	tetrabutylammonium tetrafluoroborate
R	alkyl group
M	molar concentration
EC, ECE, etc.	electrode reaction followed by chemical reaction, etc.
E_λ	switching potential
V	volt
Fp	$CpFe(CO)_2$
Fp*	$Cp^*Fe(CO)_2$
Mp	$CpMo(CO)_3$

CHAPTER 1

1.1 Overview

The use of electrochemical techniques in probing mechanistic routes of reactions of metal complexes has been much less studied when compared to that of organic reactions over the past few decades.[1] Most of the initial electrochemical studies performed on transition metal systems were confined to investigations of the reversibility of a voltammetric wave or to changes in oxidation states. The important role of electron-transfer reactions[2-5] in organotransition-metal chemistry has only been recognized in the last ten years or so, even though the ferrocene-ferrocenium electrochemical couple was discovered as long ago as the 1950's.[6]

Earlier work by Dessy and co-workers[7-12] on organometallic complexes centred on cathodic processes from which evolved the generalised[7,8] modes of reactions of these complexes upon electrochemical reductions in non-aqueous media.

The organometallic grouping RMX (where M is a metal, R is an alkyl or aryl moiety, and X is another R group or another ligand) was considered to undergo several possible reactions[7] after initial reduction, as outlined in Scheme I-1.

The anionic radical (1), which is produced on reduction of the substrate RMX, may be stable or may react to form the neutral radical (2). This radical may then react to form new organometallic species (equation I-2) or abstract hydride from the solvent to yield the hydride, (3) (equation I-3). Further reduction of (2) produces the anion RM^- (equation I-4) which may also react to form (3).

$$RMX \xrightarrow{+e^-} \underset{(1)}{RMX^{\bullet -}} \longrightarrow X^- + \underset{(2)}{RM^{\bullet}} \qquad \text{...I-1}$$

$$2RM^{\bullet} \longrightarrow RMMR \text{ (or } RMR + M^{\bullet}) \qquad \text{...I-2}$$

$$RM^{\bullet} \xrightarrow{H^{\bullet}} \underset{(3)}{RMH} \qquad \text{...I-3}$$

$$RM^{\bullet} \xrightarrow{+e^-} RM^- \xrightarrow{+H^+} (3)$$

SCHEME I-1

Many of these processes would be relevant to catalytic reactions involving transition metal alkyl intermediates.

In early studies, most of the polarographic waves for organometallic complexes were reported as irreversible processes.[7-12] The combination of this information with that obtained from cyclic voltammetry, controlled potential electrolysis and ultraviolet spectroscopy has enabled the reductive behaviour of many organometallic compounds to be explained.

As a result of their studies, Dessy and co-workers formulated a general approach[8] to survey a particular compound. This involves the following:

1. Polarographic examination;

2. Multiple triangular sweep studies (i.e. cyclic voltammetry) to establish reversibility of the system, chemically or electrochemically;

3. Controlled potential electrolysis at the required potential and the determination of n, the number of electrons involved in the polarographic step;

4. Polarographic study of the resulting solution;

5. Electron spin resonance studies at this point if warranted;

6. Attempted re-oxidation (or reduction) of the electrochemically generated species to the initial compound;

7. Polarographic and spectroscopic studies of this final solution to compare with the initial solution.

Development of more sophisticated equipment[13] has enabled transient electrogenerated species with lifetimes of ≈ 20 ns[14] to be characterized electrochemically. Voltammetric measurements of chemical systems thus unquestionably promise to be highly informative and have thus become an irreplaceable tool in the study of metal complexes in recent times.

1.2 Introduction

Electrochemical studies on chemical systems have in general dealt with the measurement of, and the relation between current and potential.[15,16] This enables the relation between the reaction rate (from the measured current) and a thermodynamic driving force parameter (from the potential) to be established.

Chemical reactions very often proceed via electron transfer steps which may be preceded and followed by chemical processes.[16-19] These charge transfer processes, however, seldom take place as simple steps and are frequently coupled to chemical reactions.

For organic and organometallic molecules, complex sequences of these processes are often proposed to describe an overall electrochemical redox reaction. A variety of characteristic chemical processes are encountered as steps in organic and organometallic electrode reactions[20] and may include protonation or deprotonation, bond cleavage, complexation or decomplexation, ligand exchange[21,22] nucleophilic or electrophilic attack, polymerization, isomerisation, or conformational change.[23]

Various electroanalytical techniques[24] have been developed in recent decades of which cyclic voltammetry (CV)[17,19,25] is the most well-used and versatile method for studying electrochemical reactions. Special characteristics of this technique are:

(a) Peak currents can be used for quantitative analysis of the electroactive species;

(b) Voltage measurements corresponding to the peaks can be used to aid identification of species being electrolysed;

(c) A number of different species can be determined in a single scan if the E-values are far enough apart;

(d) It is relatively fast; a voltammogram takes of the order of seconds or minutes to run.

The general set-up of the cyclic voltammetry apparatus (Figure I-1) comprises of a three electrode system. These electrodes are immersed in an unstirred solution of the compound. A voltage is applied to the "working electrode" and is varied linearly from an initial value, E_i. When the switching potential, E_λ, is reached, the direction of the sweep is reversed until the potential returns linearly to its initial value.

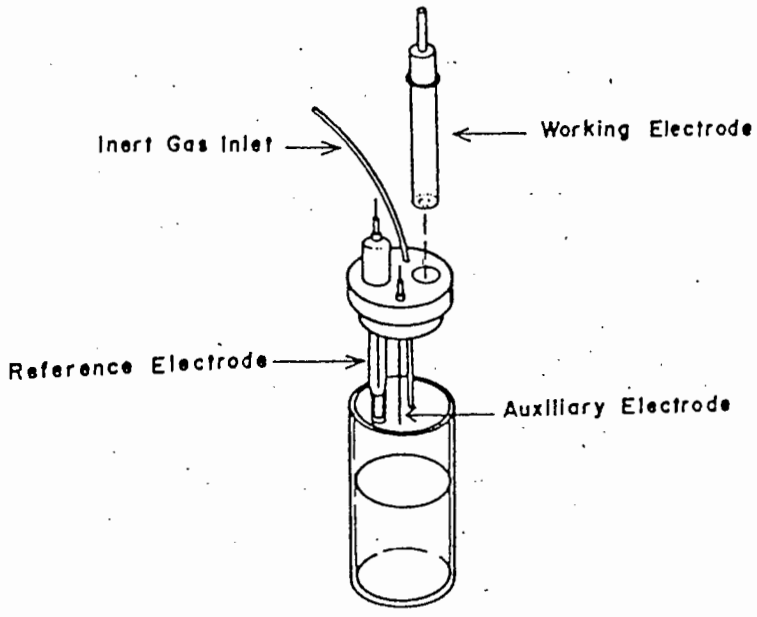

(a) Electrochemical Cell

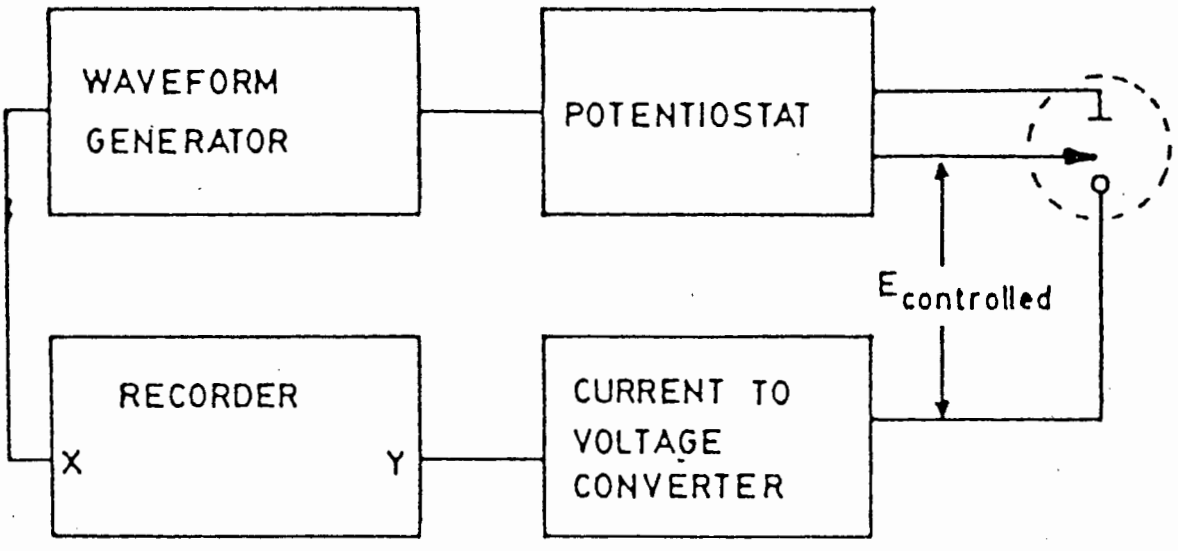

(b) Instrumentation

(Cell designation: ⟵ reference electrode; ⊥ working electrode; o— auxiliary electrode)

Figure I-1. THE CYCLIC VOLTAMMETRY APPARATUS.

(Taken from reference 25)

Charge flows between the working and inert auxiliary electrodes, while an external potentiostat monitors the potential difference between the working and reference electrodes. The resulting voltammogram thus represents the current response as a function of the applied potential.

The potential applied between the working and the reference electrode is varied with time in a typical saw-tooth wave form as shown in Figure I-2a. At the starting potential no electrode reaction occurs, and the scan is initiated towards values positive enough to effect the oxidation of the material being studied (Figure I-2a). Those species at the surface of the working electrode will undergo oxidation, and electrons will flow from the solution to the electrode, resulting in an anodic current. This faradaic current depends on (i) the rate at which the species are brought from the bulk of the solution to the electrode (mass transport), and (ii) the rate at which electrons are transported from the solution to the electrode (charge transfer).

The three modes by which mass transport can take place, are

(i) migration - movement of charged species due to the presence of an electric field,

(ii) convection - movement of species contained in a volume of stirred solution.

(iii) diffusion - movement of species along a concentration gradient.

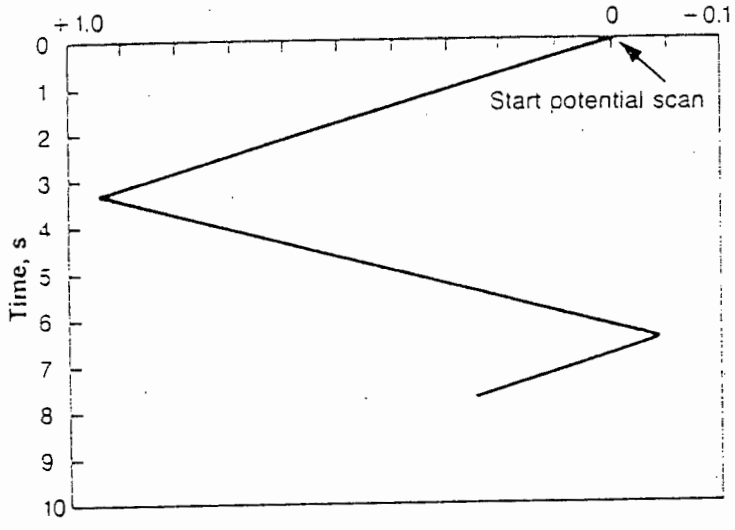

Figure I-2a The saw-tooth waveform.[a]

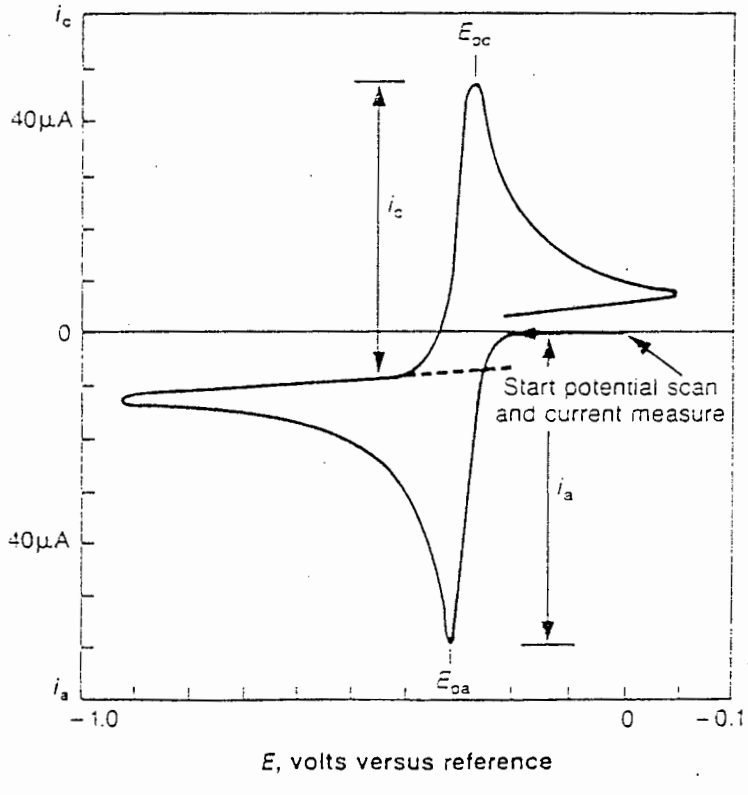

Figure I-2b. A typical cyclic voltammogram.[a]

[a]*Taken from ref. 26.*

The first two modes of mass transport are repressed by the addition of a supporting electrolyte and to keep the solution quiescent. The anodic current is therefor controlled by the rate of diffusion of the oxidisable species towards the electrode surface. A maximum current is eventually reached afterwhich it falls off due to the depletion of the species at the surface. The scan direction is reversed at the switching potential, and the diffusion-controlled cathodic current is observed. In this case electrons flow from the electrode and reduce the oxidised species produced in the forward scan. A typical curve is obtained over the entire cycle of forward and reverse sweeps (Figure I-2b).

Several important parameters characterise a cyclic voltammogram:

(i) the anodic (E_{pa}) and cathodic (E_{pc}) peak potentials,

(ii) the anodic (i_{pa}) and cathodic (i_{pc}) peak currents,

(iii) the half-wave potential $E_{½}$, defined as

$$E_{½} = \frac{E_{pc} + E_{pa}}{2}$$

The criterion for reversibility (over a given range of conditions) is that

(i) $\Delta E = E_{pa} - E_{pc} = 59/n$ mV (n = number of electrons involved in charge transfer process), which should be independent of concentration and scan rate.

(ii) the peak current is

$$i_p = (2.69 \times 10^5) n^{3/2} A D_o^{1/2} v^{1/2} C_o^*$$

where A = electrode surface (cm^2), D_o = diffusion coefficient ($cm^2\ s^{-1}$), υ = scan rate ($V\ s^{-1}$) and C_o^* = concentration (mole cm^{-3}).

Besides thermodynamic data[27] which can be obtained from precise CV measurements, mechanistic analyses can be made regarding electrode reactions including both homogeneous and heterogeneous charge transfer steps as well as coupled chemical processes.[20] Furthermore, since the sweep rate can technically be increased up to $10^6\ V\ s^{-1}$,[28-30] the time scale of the experiment can be controlled, giving insight into the kinetics of these processes.

Modified potential wave forms[31-33] can also be used to resolve mechanistic ambiguities.

Spectroscopic techniques used *in situ* with voltammetric methods enable identification of intermediates in electrolytic reactions.[15] Various spectroelectrochemical methods have been developed[34] and applied successfully for observing and identifying electrogenerated species within an electrochemical boundary of less than 5 μm.

The synthetic use of charge transfer reactions of organotransition-metal complexes has become an important tool in recent years, in that otherwise inaccessible complexes can be synthesized via routes that are fast, efficient and

stereo- or regioselective.[5,35-39] Redox activation of the metal centre has led in some cases to the synthesis of new species[36,38]. In addition, new information can be obtained about the behaviour of known or proposed catalytic intermediate species, such as metal alkyls, in important reactions such as the alkyl migration reaction.

An overview of some of the known redox systems investigated up to now will be given in the ensuing sections. This includes the well-known ferrocene-ferrocenium system, effect of ligands on metal complexes, and more specifically metal carbonyl complexes.

1.3 Ferrocene - ferrocenium system

The redox behaviour of ferrocene, bis(cyclopentadienyl)iron(II), using DC polarography and controlled potential coulometry, was first investigated by Page and Wilkinson[6] They reported a reversible one-electron oxidation of the molecule in a 90 % ethanol solution at a dropping mercury electrode to form the ferricinium ion. The halfwave potential of this couple (equation I-5) was measured at +0.31 V *versus* the standard calomel electrode.

$$(C_5H_5)_2Fe \rightleftharpoons [(C_5H_5)_2Fe]^+ + e^- \qquad \text{...I-5}$$

Investigations into the electrochemical behaviour of ferrocene in different solvents soon followed, establishing the highly reversible nature of the heterogeneous electron charge transfer process with its corresponding halfwave potential.[40-43] Redox potentials of ferrocene-derivatives[41,45-48] show that oxidation takes place at more positive potentials for electron-withdrawing substituents. This enabled a correlation to be drawn between quater-wave potentials and Taft σ constants for substituted phenylferrocenes.[49]

The electrochemical properties of the ferrocene-ferrocenium couple has led to it being used as a standard for comparison of measured potentials in various solvents. The required properties of such a standard were determined as:[44]

(a) Both halves of the couple should be soluble, and should further

(b) Have a small charge and large ionic radii;

(c) Be spherical;

(d) Undergo rapid and reversible redox reaction;

(e) Be reasonably soluble in suitable solvents, and not undergo chemical or structural changes upon the charge transfer process;

(f) Not have strong oxidizing or reducing power.

1.4 Ligand 0Effects On Electrochemical Behaviour In Metal Complexes.

The electrochemical parameter E° (standard reduction potential) is indicative of the energy difference between two oxidation states. This thermodynamic property is directly measurable or determined from polarographic voltammetric measurements for reversible electrode processes. Factors such as *substituent effects* which have an influence on $E_{1/2}$ or E° may thus be readily interpreted, provided the electrode processes are *diffusion controlled.* More complex situations arise when dealing with non-Nernstian conditions (i.e. where the electrode process is determined by the rate of a chemical or electron-transfer step) since the corresponding $E_{1/2}$ measurement reflects both thermodynamic and kinetic information.

For metal complexes, ML_n, the electron-withdrawing or electron-donating ability of the ligand, L, is reflected in the properties of the complex, and is determined by the flow of electron density from the metal orbitals into the ligand orbitals (back bonding) and the counter flow from ligand σ, $p\pi$ or $d\pi$ orbitals onto the metal. These compounds can conveniently be classified according to their coordinated ligands. The types of reactions these compounds

undergo are often determined by the nature of the metal-ligand bond.[50] Ligands are divided into two main classes[51] which reflect their mode of bonding:

(i) simple donor ligands, eg. NH_3, halides

(ii) π-bonding or π-acid ligands, eg. CO, PPh_3

Also, depending on their ability to form multiple bonds, simple donor ligands can supplement their σ-bonds by π interaction.
The electronic environment of the central metal is thus dependent upon the nature of the metal-ligand bond.

The oxidation potential of a metal complex is related to the energy of the highest occupied molecular orbital (HOMO).[52-54] Two ways[55] of metal-ligand interaction can lower the energy of this level and consequently lead to less anodic oxidation potentials:

(i) since the energy of the electrons occupying these orbitals is influenced by the effective nuclear charge on the metal, net donor ligands will bring about more effective screening of these electrons;

(ii) conjugation of the ligand orbitals with the HOMO.

Chatt *et al*[55] reported the one-electron oxidation of $[Cr(CO)_5L]$ to be very sensitive to the nature of L. The ligand constant, P_L (equation I-6), has more positive values for ligands having weak σ-donor and strong π-acceptor properties (such as N_2^+, NO^+ and CO) and more negative values for ligands having strong σ- and π-donor properties (e.g. Cl^-, OH^-).

$$P_L = E^{ox}_{½}[Cr(CO)_5L] - E^{ox}_{½}[Cr(CO)_6] \qquad \text{...I-6}$$

These constants thus represent the change in the energy of the HOMO of $Cr(CO)_6$ when a CO ligand is replaced by L.

Various attempts to utilize the electrochemical potential of metal complexes to resolve the σ- and π-components of transition metal-tertiary phosphine bonding and to classify these ligands as σ-donor/π acceptor ligands have been reported.[44,45,50,51] Giering *et al*,[59-61] for example, successfully applied these data to interpret the kinetics and mechanisms of the redox-promoted carbonylation of Cp(CO)(L)FeMe as a function of the nature of L (L = tertiary phosphine ligands).

1.5.1 Stereo-Electronic Effects Of Tertiary Phosphine Ligands.

Changing substituents on tertiary phosphine ligands causes changes in the kinetics and mechanisms of reactions involving transition metal tertiary phosphine complexes.[56,62-65] These ligands are thought to involve two intimately related components,[66] viz.

electronic effects, which are a measure of change due to the electronic transmission along a chemical bond;

steric effects, which are a measure of change due to (usually) non-bonding forces between parts of a molecule.

Attempts to quantify these effects were first done by Tolman[66] by introducing the cone angle (θ, steric parameter) and χ-values (electronic parameter). The proposed electronic parameter was based on substituent contributions, χ_i, which were derived from the CO stretching frequency belonging to the A_1 mode of the complexes, $Ni(CO)_3L$ (L = tertiary phosphine ligands).

In general, the electronic properties of phosphorus ligands are divided into σ-donor ability and π-acidity.[67] Tolman's χ-values are thought to reflect the net electron donor/acceptor properties of the ligands and include both σ- and π-effects.

It has been shown[56] that the oxidation potentials of a series of manganese complexes, $(MeC_5H_4)Mn(CO)_2L$ (L = triaryl or mixed aryl/alkyl phosphine ligands) are linearly related to the basicities (pK_a values) of the ligand L. The complexes with less basic phosphorus(III) ligands are more difficult to oxidise, while those containing the highly electron rich trialkylphosphines were oxidized at less anodic potentials. The ease of oxidation of these complexes is directly related to the strength of the σ-donor ability (χ-values) of the ligands.

The electron density on the metal centre is strongly influenced by the nature of the phosphine ligand, which in turn depends on the type of groups attached to the phosphorus atom. Thus, strong σ-donors (low χ-values) will increase the electron density whereas strong π-acids will decrease the electron density. Also, the terminal carbonyl stretching frequencies of the complexes CpFe(CO)(L)(COMe) (L = phosphorus(III) ligands) would be directly related to the electron density on the metal to which the carbon monoxide is bonded.

For metal carbonyl complexes containing pure σ-donors, plots of ν(CO) (cyclohexane) against the oxidation potential (MeCN, 0 °C) of these acyl complexes showed a linear relationship[58]: complexes having higher CO stretching frequencies are more difficult to oxidize. Thus, the electrochemical

oxidation potential is a useful tool to determine the extent of electron density on the metal. Similar observations were made for the complexes Cp'Fe(CO)(L)Me.[58]

Giering *et al*[56-58] have attempted to quantitatively resolve the ligand effects of the metal-PR_3 bond into σ- and π- components by correlating Tolman's electronic parameters (χ) of phosphorus(III) ligands with the oxidation potentials of the corresponding manganese complexes,[56] $Cp'Mn(CO)_2L$.

The pKa values of the conjugated acids of all the phosphorous bases (Table I-1) showed a remerkable linear correlation with the E° values of these manganese complexes. Since the pKa value increases with decreasing basicity of the corresponding phosphorous base, it serves as a suitable parameter for the electron donor ability of the phosphorous ligand. These ligands were consequently grouped as "pure σ-donors". These ligands are also known to have low π-acceptor ability[65]. The ease of oxidation thus reflects the σ-donor strength only.

Table I-1. Standard reduction potentials[a] for $Cp'(CO)_2MnL$.

Substituent L	E°[b] (V)	$\nu(CO)$[c] (cm^{-1})
PPh_3	0.51	2068.9
P(*p*-MePh)$_3$	0.49	2066.7
P(*p*-MeOPh)$_3$	0.478	2066.1
$PEtPh_2$	0.475	2066.7
$PMePh_2$	0.472	2067.0
$PBuPh_2$	0.47	-
PEt_2Ph	0.444	2063.7
PMe_2Ph	0.436	2065.3
PMe_3	0.400	2064.1

[a] *Taken from reference 56.* [b] *Acetonitrile, -45°C, vs SCE, 200 mV* s^{-1}.

[c] *Values for* $Ni(CO_3)$, *taken from reference 66.*

The trend of potential values is in agreement with work done by Puddephatt *et al*[69] who established that methyl groups increase the donor ability of phosphine ligands, compared to phenyl groups.

Other manganese complexes studied[56] were found to be either more or less difficult to oxidize than predicted by their corresponding pK_a values and were

grouped as such. The class of compounds which is more difficult to oxidise thus contains those phosphorus ligands having an overall poorer electron donor ability and this was suggested to be the onset of the π-acids. Thus, their σ-donor strength is diminished by back bonding into the d-orbitals of the ligand, effectively reducing the electron density on the metal.

The class of compounds which is less difficult to oxidise (π-bases) experiences an enhanced electron density (from σ-donor and π-donor effects) on the metal centre, thereby easing the oxidation process. The corresponding ligands were classified as π-bases.

1.5.2 Correlation of E° and ν(CO) for CpFe(CO)L(COMe), Cp'Fe(CO)L(COMe) and CpFeL(CO)Me.

The carbonyl stretching frequencies of the single terminal carbonyl group for the complexes CpFe(CO)L(COMe), Cp'Fe(CO)L(COMe) and CpFeL(CO)Me were analysed[58] as a function of the formal reduction of these complexes. In each case, for plots of stretching frequencies against the formal reduction, a linear relationship was obtained and the ligands were divided into two characteristic groups: one having a steeper slope and showing more scattering than the other. The model[63] proposed to separate the σ-donor and σ-donor/π-acceptor ligands was that for the same family of complexes, the property of formal reduction should be linearly related to the σ-donicity (σ_d) and π-acidity (π_a) (equations I-7 and I-8) of the ligands.

Thus, for σ-donor ligands,

$$E° = a\sigma_d + b \qquad \text{...I-7}$$

and for π-acceptor ligands

$$E^\circ = A\sigma_d + B\pi_a + C. \qquad \text{...I-8}$$

(a, B, etc. are constants)

Based on the above equations, plots of E° against ν(CO) will show less scattering (apart from experimental error) for complexes containing σ-donor ligands than for those containing ligands exhibiting both σ- and π-effects. Experimentally obtained results[58] (Tables I-2 to I-4) were resolved using these criteria and ligands could thus be tabulated according to their qualitatative donor abilities.

Table I-2. Reduction potentials and ν(CO) for CpFe(CO)L(COMe) : (L = σ-donor tertiary phosphines)[a].

Substituent L	ν(CO)[b] (cm^{-1})	E°[c] (mV)
$P(p\text{-}Me_2NPh)_3$	1913.2	0.189
$P(i\text{-}Bu)_3$	1914.1	0.202
PEt_3	1916.6	0.219
PBu_3	1915.1	0.222
$PMe(i\text{-}Bu)_2$	1916.0	0.242
PEt_2Ph	1917.6	0.248
$PCyPh_2$	1917.0	0.257
PMe_2Ph	1918.7	0.274
$P(p\text{-}MeOPh)_3$	1919.0	0.276
$P(p\text{-}MePh)_3$	1920.0	0.280
PPh_3	1922.0	0.322
$PPh_2(CH_2CH_2CN)$	1924.0	0.347
$P(p\text{-}FPh)_3$	1924.0	0.361
$P(OEt)Ph_2$	1926.0	0.375
$P(p\text{-}ClPh)_3$	1926.0	0.380
$P(OMe)Ph_2$	1926.1	0.383
$P(p\text{-}CF_3Ph)_3$	1929.4	0.439

[a] *Taken from reference 58.*
[b] *Cyclohexane.*
[c] *vs SCE, in CH_3CN (0.2 M $LiClO_4$), at O °C.*

Table I-3. Reduction potentials and ν(CO) for Cp'Fe(CO)L(COMe): L = σ-donor ligand[a].

Substituent L	ν(CO)[b] (cm^{-1})	E°[c] (mV)
$P(p\text{-}Me_2NPh)_3$	1909.0	0.159
$P(i\text{-}Bu)_3$	1910.0	0.174
PEt_3	1912.0	0.178
$PMe(i\text{-}Bu)_2$	1911.9	0.197
PBu_3	1911.0	0.202
PEt_2Ph	1913.0	0.216
$PCyPh_2$	1911.0	0.225
PMe_2Ph	1914.4	0.236
$P(p\text{-}MeOPh)_3$	1915.0	0.259
$P(p\text{-}MePh)_3$	1916.0	0.266
PPh_3	1918.0	0.297
$PPh_2(CH_2CH_2CN)$	1919.0	0.319
$P(p\text{-}FPh)_3$	1920.0	0.356
$P(OMe)Ph_2$	1922.9	0.358
$P(OEt)Ph_2$	1922.0	0.358
$P(p\text{-}ClPh)_3$	1921.0	0.366
$P(p\text{-}CF_3Ph)_3$	1924.4	0.412

[a] *Taken from reference 58.*
[b] *Cyclohexane.*
[c] *vs SCE, in CH_3CN (0.2 M $LiClO_4$), at O °C.*

Table I-4. Reduction potentials and ν(CO) for CpFe(CO)LCOMe: L = σ-donor ligand.[a]

Substituent L	ν(CO)[b] (cm^{-1})	E° [c] (mV)
$P(p\text{-}Me_2NPh)_3$	1912.7	0.149
PEt_3	1915.0	0.152
PBu_3	1914.0	0.156
$PMe(i\text{-}Bu)_2$	1914.1	0.191
PEt_2Ph	1915.4	0.213
PMe_2Ph	1916.8	0.217
$P(p\text{-}MeOPh)_3$	1915.0	0.250
$P(p\text{-}MePh)_3$	1917.1	0.285
PPh_3	1920.0	0.302
$P(p\text{-}FPh)_3$	1922.1	0.338
$PPh_2(CH_2CH_2CN)$	1918.6	0.345
$P(OMe)Ph_2$	1920.0	0.352
$P(OEt)Ph_2$	1919.2	0.355
$P(p\text{-}ClPh)_3$	1924.0	0.385

[a] *Taken from reference 58.*
[b] *Cyclohexane.*
[c] *vs SCE, in CH_3CN (0.2 M $LiClO_4$), at O °C.*

1.6 Electrochemical behaviour of some cyclopentadienyl iron carbonyl alkyl compounds.

Electrochemical studies on organometallic compounds have, apart from the synthetic applications[5], drawn much interest because of the subsequent reactions these species undergo upon electrochemical activation. The alkyl migratory CO insertion reaction, (equation I-9) being a key step in many catalytic transformations, is among the most studied of chemical processes,[70,71] both chemically[72-89] and electrochemically.[59-61,90-95]

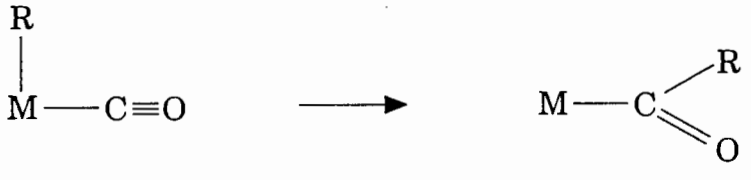

...I-9

The oxidation of iron carbonyl alkyl compounds, which has been found to initiate and enhance the alkyl migration process, has received much attention.[59-61,90-95] These investigations were mainly done

(a) in solvents of different donor strengths to investigate solvent dependence of the mechanism;

(b) under varying scan rates to investigate the kinetics of the redox processes, and also the reversibility thereof;

(c) at sufficiently low temperatures to slow down the reaction rates to facilitate the characterisation of reaction intermediates.

Magnuson *et al*[91] have characterised an intermediate 17e⁻ radical cation (**5**, Scheme I-2) which was generated by one-electron chemical oxidation of $CpFe(CO)_2Me$ (**4**) using ceric ammonium nitrate (CAN) or anhydrous cupric triflate (equation I-10).

$$CpFe(CO)_2CH_3 \rightarrow [CpFe(CO)_2CH_3]^+ + e^- \quad \text{...I-10}$$

(4) (5)

$$[CpFe(CO)_2CH_3]^+ + MeCN \rightarrow [Cp(CO)(MeCN)FeCOCH_3]^+ \quad \text{...I-11}$$

(5) (6)

SCHEME I-2

In acetonitrile at -20 °C the resulting deep green solution was shown to contain the solvent incorporated cation $[Cp(CO)(MeCN)Fe(COCH_3)]^+$ (**6**), with a reported half life of 22 seconds. Similar results were obtained by chemical

oxidation of the acyl complexes $Cp(CO)(L)Fe(COCH_3)$ (L = CO, PPh_3), to give the acetyl cation, $[Cp(CO)(L)Fe(COCH_3)]^+$.

Thus, the oxidation of $CpFe(CO)_2CH_3$ is followed by a rapid methyl migration (Scheme I-2, equation I-11). Cyclic voltammetric studies have shown that the anodic wave of (**4**) is irreversible at scan rates of up to 10^5 mV s^{-1}. This means that upon scan reversal (that is after the initial anodic wave has been swept), virtually none of the radical cation (**5**) is present, since virtually all has been transformed to the acetyl cation (**6**) via methyl migration. The irreversibility of the oxidation wave at such high scan rates thus gives an insight into the enormous rate enhancement of the alkyl migration step upon oxidation of the iron-alkyl compound (**4**).

Upon further investigation,[92] the oxidation of complexes of the type $Cp(CO)(L)FeCH_3$ (**7**, L = PPh_3, P(*i*-PrO)$_3$ **4**, L = CO) was studied in weakly coordinating solvents such as acetone and dichloromethane at 0 °C. Under these conditions, the cation $[Cp(CO)(L)FeCH_3]^+$ (**8**, Scheme I-3), was observed electrochemically.

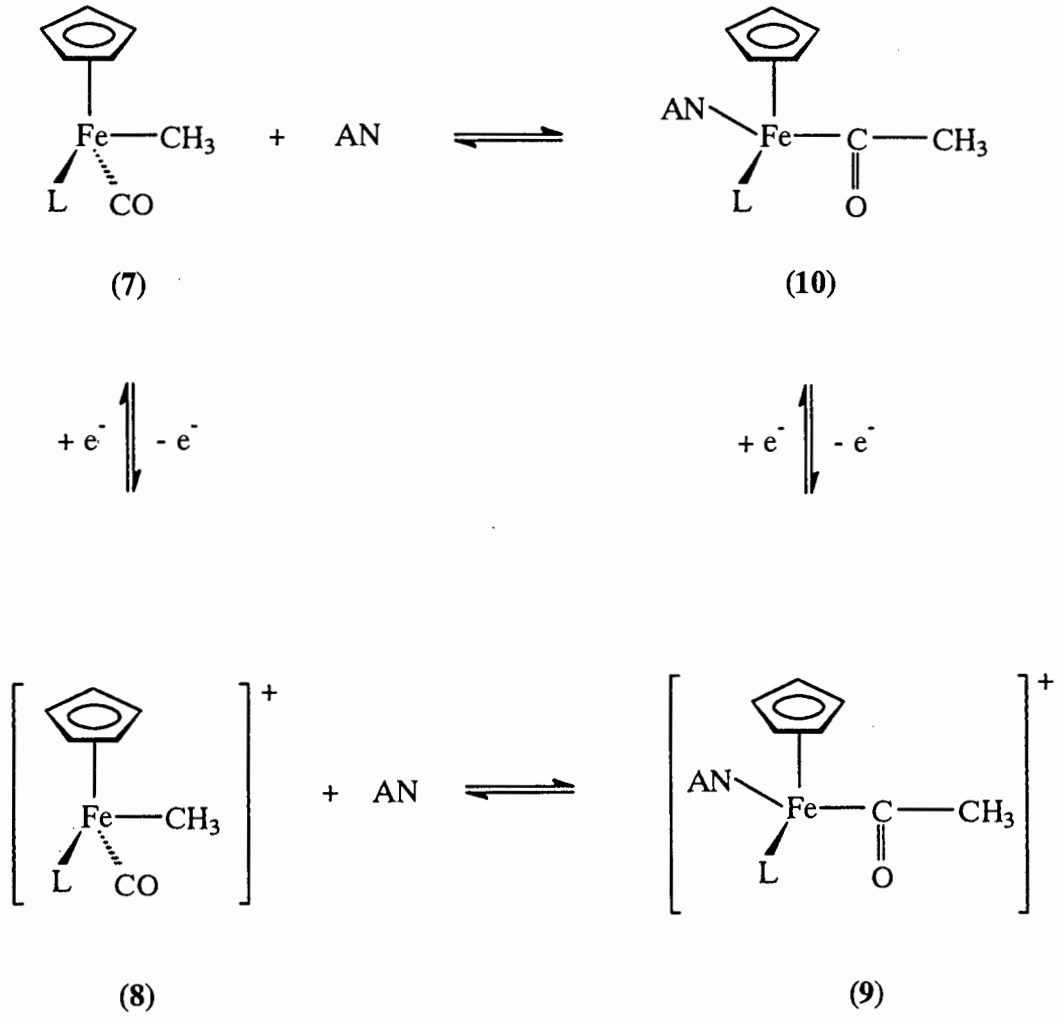

SCHEME I-3

Cyclic voltammograms of (7) showed the appearance of a cathodic wave which is coupled to the initial oxidation wave to present a quasi-reversible oxidation process. Thus, in the absence of a strong nucleophilic solvent, the formation of the solvent incorporated acyl cation $[Cp(CO)(L)(S)Fe(COCH_3)]^+$ (S = solvent), is

excluded and the generated $[Cp(CO)(L)FeCH_3]^+$ is reduced electrochemically to again form the neutral compound, (7).

With increasing amounts of the stronger nucleophilic solvent, acetonitrile, the reduction wave of $[Cp(CO)(L)FeCH_3]^+$ is steadily suppressed with the simultaneous appearance of a new reduction wave at more negative potentials. This new cathodic wave was attributed to the reduction of $[Cp(L)(MeCN)Fe(COCH_3)]^+$ (9), to form $Cp(L)(MeCN)Fe(COCH_3)$, (10).

What is of importance in the mechanism is that for the rate enhancement of the alkyl migratory insertion step for the iron alkyl compound (7), one-electron oxidation is not the only requirement. The presence of a nucleophile, in this case the solvent acetonitrile, is needed and is suggested to be coordinated to the metal of the acyl cation (9). It was also found that in the cyclic voltammograms of these iron alkyl species, the presence of cation (8) was observed in cycles with scan rates of up to 20 V s^{-1}. The equilibrium constant for the migratory insertion (8) $\rightleftharpoons$ (10) is reported[91] to increase a trillion fold compared to that undergone by the neutral 18e parent complex, (7) $\rightleftharpoons$ (10).

The reduction wave of $[Cp(L)(MeCN)Fe(COCH_3)]^+$ (9) was found to be coupled to a quasi-reversible anodic wave. Repeated cycles over this couple indicated

chemical decomposition of the neutral complex, Cp(L)(MeCN)Fe($COCH_3$). This is attributed to the decarbonylation step to reform the starting complex (7).

Golovin *et al*[93] investigated the electrochemical and chemical oxidation of the complex Cp'$(CO)_2$FeMe (11), in mixtures of methanol and acetonitrile (Scheme I-4).

$$Cp'(CO)_2FeMe \rightleftharpoons [Cp'(CO)_2FeMe]^+ + e^-$$

(11) (12)

$$[Cp'(CO)_2FeMe]^+ + MeOH \rightarrow [Cp'(MeOH)(CO)Fe(COMe)]^+ \quad \text{...I-12}$$

(13)

$$[Cp'(CO)_2FeMe]^+ + MeCN \rightarrow [Cp'(CO)(MeCN)Fe(COMe)]^+$$

$$[Cp'(CO)(MeOH)Fe(COMe)]^+ + MeCN \rightleftharpoons [Cp'(CO)(MeCN)Fe(COMe)]^+ + MeOH \quad \text{...I-13}$$

$$[Cp'(MeOH)Fe(COMe)]^+ + e^- \rightleftharpoons Cp'(MeOH)Fe(COMe) \quad \text{...I-14}$$

$$[Cp'(CO)(MeCN)Fe(COMe)]^+ + e^- \rightleftharpoons Cp'(CO)(MeCN)Fe(COMe) \quad \text{...I-15}$$

SCHEME I-4

Cyclic voltammograms (CV's) of $Cp'(CO)_2FeMe$ at -45 °C in neat methanol showed that it was oxidised irreversibly at 1.25 V (*vs.* SCE), followed by a reversible couple at -0.03 V which was assigned to the redox reaction as in Scheme I-4 (equation I-14).

Identical CV's were obtained for solutions that were oxidised chemically with 0.8 molar equivalents of CAN. IR spectroscopy on the resulting solution of $[Cp'(CO)(MeOH)Fe(COMe)]^+$ (**13**) showed a strong absorption band at 1605 cm^{-1}, in agreement with the similar complex, $[Cp(CO)(MeCN)Fe(COMe)]^+$.[91]

The reduction of $[Cp'(CO)_2FeMe]^+$ (**12**), in methanol or ethanol could not be observed electrochemically, even at a temperature of -34 °C and scan rate of 1 V s^{-1}, due to its fast transformation to the acyl complex.

Two redox couples (0.1 V and -0.07 V) appeared in CV's of solutions at -34 °C containing (**12**) in methanol to which acetonitrile was added. These coupled waves were assigned to the redox processes of $[Cp(CO)(MeOH)Fe(COMe)]^+$ (equation I-14) and $[Cp'(CO)(MeCN)Fe(COMe)]^+$ (equation I-15) which was formed after the initial chemical oxidation of $Cp'(CO)_2FeMe$ with CAN. It was found that the ratio of the reduction currents (i_{MeCN} / i_{MeOH}) reflects the relative concentrations of the two solvents. Furthermore, the interconversion of $[Cp'(CO)(MeCN)Fe(COMe)]^+$ and $[Cp'(CO)(MeOH)Fe(COMe)]^+$ (equation I-13), was followed by reverse pulse voltammetry. This indicated second-order

kinetics with a rate constant of $k = 5 \times 10^{-3}$ M^{-1} s^{-1}, favouring the acetonitrile complex. The formation of both complexes was found to occur with approximately equal rate constants. These constants have large values at temperatures as low as -34 °C since the reduction of $[Cp'(CO)_2FeMe]^+$ (**12**) could not be observed in mixtures of these solvents, implying a highly reactive electron deficient species.

Trogler and Therien[94] used transient electrochemical techniques in combination with spectroscopic studies to show that the cation, $[CpFe(CO)(PPh_3)CH_3]^+$ (**15**), resulting from the one-electron oxidation of $CpFe(CO)(PPh_3)CH_3$ (**14**), undergoes nucleophilic attack at the 17e⁻ metal centre to form the 19e⁻ transition state (**16**), (Scheme I-5) .

$$CpFe(CO)(PPh_3)CH_3 \rightleftharpoons [CpFe(CO)(PPh_3)CH_3]^+ + e^-$$

(**14**) (**15**)

$$[CpFe(CO)(PPh_3)CH_3]^+ + L \rightleftharpoons [CpFe(CO)(PPh_3)(L)CH_3]^+$$

(**16**, L = pyrridine)

$$[CpFe(CO)(PPh_3)(L)CH_3]^+ \rightleftharpoons [CpFe(PPh_3)(L)(COCH_3)]^+ \quad \ldots I\text{-}16$$

SCHEME I-5

This hypervalent intermediate $[CpFe(CO)(PPh_3)(L)CH_3]^+$ (L = incoming ligand), was found to be a direct precursor to the acyl species $CpFe(PPh_3)(L)(COCH_3)$, in the alkyl to acyl migratory insertion reaction.

The cyclic voltammogram of (14) in CH_2Cl_2 at 0 °C (scan rate = 200 mV s^{-1}) with an added 200 molar excess of pyridine showed, after the initial oxidation wave, the appearance of a new reduction wave prior to the potential required to reduce the 19e⁻ cation (16). Also, under these conditions the oxidation of the iron-alkyl compound (14) becomes reversible.

The new cathodic peak at -290 mV (vs Ag wire pseudo-reference electrode) could also be observed at room temperature at scan rates of between 2.5 to 15 V s^{-1} and was attributed to the reduction of $[CpFe(CO)(PPh_3)(py)CH_3]^+$: (equation I-17)

$$[CpFe(CO)(PPh_3)(py)CH_3]^+ + e^- \rightleftharpoons CpFe(CO)(PPh_3)(CH_3) + py \quad \text{...I-17}$$

(16)

Thus, during the time-scale of the cyclic voltammogram, this reduction process renders the 19e· species unavailable for the methyl migration reaction (equation I-16). At a scan rate of 15 V s^{-1} the electron transfer process involving the reduction of $[CpFe(CO)(PPh_3)(py)CH_3]^+$ takes place fast enough, that is virtually

none of it rearranges to the acyl cation and hence no cathodic wave for the reduction of the 19e⁻ acyl species is observed.

It was also shown[94] that at a particular scan rate at 0 °C, the addition of different amounts of nucleophiles was needed to produce equal currents for the reduction of $[CpFe(CO)(PPh_3)CH_3]^+$. The ratio of molar excess of nitrogen containing nucleophiles with respect to the iron-alkyl compound increases with decreasing σ-basicity:

(3,4-dimethylpyridine : pyridine : 3-chloropyridine = 60 : 200 : 5000).

Hence, increasing amounts of ligands of decreasing nucleophilicity are needed for the chemical conversion of a fixed amount of electrochemically generated (**15**) to $[CpFe(CO)(PPh_3)(py)CH_3]^+$. These nucleophiles thus stabilize the latter cation (**16**) which serves as further proof for the existence of the proposed 19e⁻ species. Cyclic voltammograms also showed, that at a constant scan rate, the CO insertion step takes place faster for the more electron rich nucleophile.

In an attempt to understand the dynamic role of the solvent in the transformation of $[Cp(CO)_2FeMe]^+$ (**5**), to $[Cp(CO)(Sol)Fe(COMe)]^+$, Giering *et al*[95] extended their investigations to the oxidation of $Cp(CO)_2FeMe$ (**4**), at low temperatures in acetone.

$$Cp(CO)_2FeMe \rightleftharpoons [Cp(CO)_2FeMe]^+ + e^-$$

(4) (5)

$$[Cp(CO)_2FeMe]^+ + S \rightarrow [Cp(CO)(S)Fe(COMe)]^+$$

(17)

$$[Cp(CO)_2FeMe]^+ + ClO_4^- \rightarrow Cp(CO)(ClO_4)Fe(COMe)$$

(4) (18)

$$[Cp(CO)(S)Fe(COMe)]^+ + e^- \rightleftharpoons Cp(CO)(S)FeMe \qquad \text{...I-18}$$

(17)

$$[Cp(CO)(ClO_4)Fe(COMe) + S \rightarrow [Cp(CO)(S)Fe(COMe)]^+ + ClO_4^-$$

(18)

S = Acetone

SCHEME I-6

It was found that the CV for (4), in acetone (0.1 M $LiClO_4$ as supporting electrolyte) at -41 °C showed a quasi-reversible couple at E° = -0.08 V (*vs.* SCE) after the initial irreversible oxidation wave (Ep = 1.20 V). This process was assigned to the oxidation and reduction of the acetone complex (17), Scheme I-6, equation I-18) and compares well with E° = -0.07 V for the methanol complex $[Cp(CO)(MeOH)Fe(COMe)]^+$.[93]

At temperatures below -35 °C, however, the appearance of a new irreversible wave at a more cathodic potential occurred, which was attributed to the reduction of the perchlorate complex, $Cp(CO)(ClO_4)Fe(COMe)$ (18). The ratio of the reduction currents for the acetone and perchlorate complexes, $i_{MeCN}/i_{perchlorate}$ was found[95] to be independent of the starting concentration of the iron-alkyl compound, but increases with decreasing scan rate. Thus, the formation of the perchlorate complex in competition with the acetone complex, despite ClO_4^- being a much poorer nucleophile than acetone (which is in 100-fold excess), indicates the high reactivity of the 17e$^-$ species $[Cp(CO)_2FeMe]^+$, which indiscriminately reacts with available nucleophiles. Also, the electrostatic forces play an important role in this particular system. The absence of $Cp(CO)(ClO_4)FeCOMe$ in earlier experiments,[93] also suggests the greater solvating power of methanol compared to acetone.

The redox-catalysed carbonylation of Cp(CO)(L)FeMe (L = tertiary phosphine ligands) was investigated[59-61] under a CO atmosphere using solvents of different nucleophilicities and mixtures thereof. These studies probed the carbonylation mechanism of the cation $[Cp(CO)(L)FeMe]^+$, using voltammetric techniques.
In methylene chloride,[59] the migratory insertion rate constants, k_{mi}, remained unaffected with changes in both substrate and CO concentrations. The rate-

determining step is suggested to be the transformation of $[Cp(CO)(L)FeMe]^+$ into a transient intermediate, followed by the rapid reaction with CO (Scheme I-7).

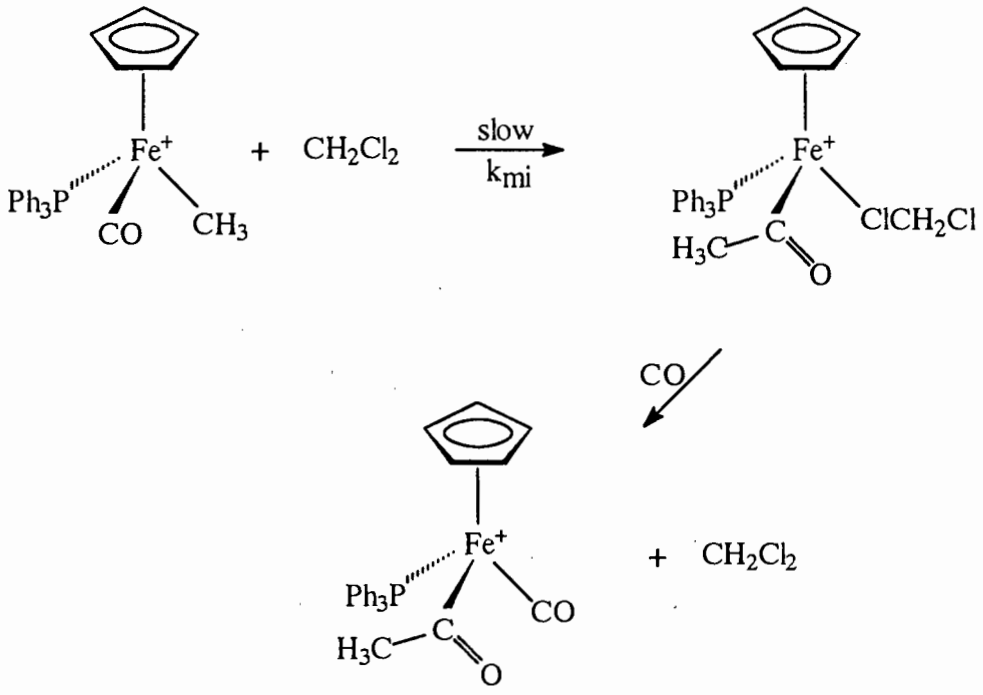

SCHEME I-7

Although the complex $[Cp(CH_2Cl_2)(L)Fe(COMe)]^+$ was not observed, thermodynamic data favoured its existence over the transient, unsaturated 15-electron complex. The subsequent reaction is thus the rate determining displacement of the solvent ligand by carbon monoxide.

In support of this, exclusive incorporation of ^{13}CO at the terminal position in $[Cp(^{13}CO)(PPh_3)Fe(COMe)]^+$ was found.

The rate of carbonylation of $[Cp(CO)(L)FeMe]^+$ was found to increase with decreasing electron-donor ability of L.

In acetonitrile (1 atm CO, 0 °C), however, the rate determining step was found[60,61] to be the reaction of CO with the solvent-coordinated acyl complex, $[Cp(MeCN)(L)Fe(COMe)]^+$. Linear sweep voltammograms enabled the equilibria of

$$[Cp(MeCN)(L)FeMe]^+ + CO \rightleftharpoons [Cp(MeCN)(L)Fe(COMe)]^+$$

were studied and was found to be dependent on the nature of the tertiary phosphine ligand. The electronic profile of K_{eq} for these equilibria showed that poorer electron donor ligands were associated with larger K_{eq}.

1.7 Kinetic studies on alkyl molybdenum carbonyl compounds of the type $CpMo(CO)_3R$.

The kinetics of the alkyl migration reaction of alkyl molybdenum carbonyl compounds have received some attention.[73,87,98-101] These investigations have mainly focused on the influence tertiary phosphines have on the rate of migration in different solvents.

The mechanism first put forward by Butler *et al*[73] (Scheme I-8) was based on kinetic measurements on the compound $CpMo(CO)_3Me$ **(19)**. They found no appreciable change in the rates of reaction of **(19)** with tertiary phosphines, L, to give the acyl complex **(21)**, using tetrahydrofuran as solvent.

The mechanism (Scheme I-8) was found to be dependent on

(i) the interaction of the solvent

(ii) the nucleophilicity of the ligand, L.

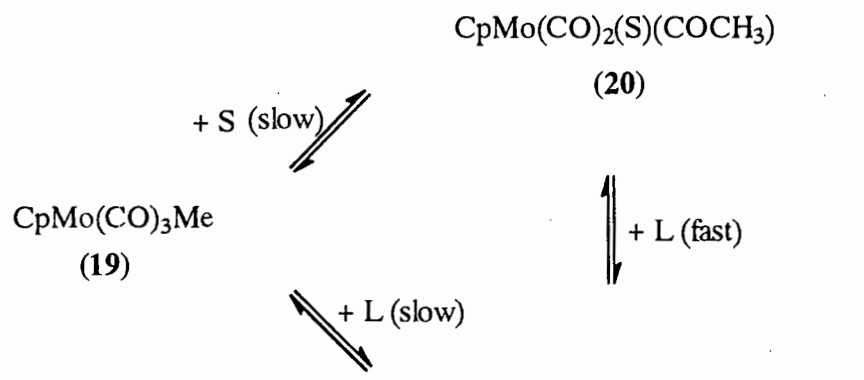

S = solvent, L = PPh_3, $P(n\text{-}C_4H_9)_3$, $P(n\text{-}OC_4H_9)_3$, $P(OC_6H_5)_3$

SCHEME I-8

The two reaction pathways thus consist of

(a) a solvent-assisted pathway whereby a polar solvent molecule induces the formation of an acyl intermediate (**20**) and which is subsequently displaced by a nucleophilic ligand;

(b) a direct attack on the metal alkyl by the nucleophile.

The rates of the alkyl migration reaction only become dependent on the concentration of L when either the nucleophilicity of L is high or the co-ordinating ability of the solvent is low, or both. The methyl migration reaction of (**19**) thus proceeds via the solvent- and/ or nucleophilic route.

Hart-Davis and Mawby[98] suggested that the ground state of $CpMo(CO)_3Me$ is hardly affected by the replacement of the cyclopentadienyl by the indenyl ligand. This observation was based on the very similar CO stretching frequencies for corresponding complexes. They found that the complex $(C_9H_7)Mo(CO)_3Me$ undergoes the carbonyl insertion reaction in the presence of tertiary phosphines via the mechanism proposed by Butler *et al*[73] (Scheme I-8). However, values obtained for the rate constant, k_1 (equation I-19), were found to be approximately 20 times faster than that for the corresponding cyclopentadienyl complex.

$$(C_9H_7)Mo(CO)_3Me + S \underset{}{\overset{k_1}{\rightleftharpoons}} (C_9H_7)Mo(CO)_2(S)(COMe) \qquad \text{...I-19}$$

S = THF

This increased reactivity of the indenyl analogue was proposed to be due to the sideways displacement (η^5 to η^3 slip) of the indenyl ligand (Scheme I-9) with

respect to the coordination site which transforms the bonding to an allyl system. The resulting vacant orbital is then available for the incoming nucleophile.

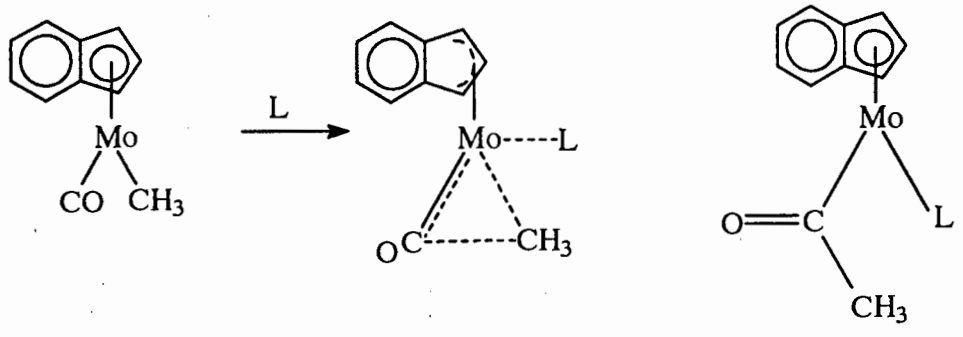

(The two CO groups not involved in the reaction have been omitted)

SCHEME I-9

The triphenylphosphine-induced alkyl migration reactions (equation I-20) of a series of benzylmolybdenum complexes have been studied extensively.[87,100 - 101]

$$CpMo(CO)_3Bz + PPh_3 \xrightarrow{MeCN} CpMo(CO)_2(PPh_3)COBz \qquad ...I\text{-}20$$

Bz = $PhCH_2$.

The variation of the rate constants for the above reaction shows[87] no correlation with Tolman's[66] electronic parameter ν (see p. 18), and decreases with increasing cone angle, θ, of the phosphine (Table I-5). This is in contrast with the $(CO)_5MnCH_2C_6H_5$ system where these constants increase with decreasing ν, i.e. with increasing electron donicity.

For several *para*- and *meta*-substituted benzyl compounds[101] of the type $CpMo(CO)_3CH_2C_6H_4X$, the rate of the CO insertion reaction increased with increasing electron-donating ability of the substituent, X. The most reactive system (*p*-methoxy) reacted approximately five times faster than the least

reactive (*p*-trifluoromethyl) complex and values obtained correlated well with the Hammet σ substituent parameters.

Table I-5. Variation of rate constants with electronic parameter, ν[a], for the reactions of $CpMo(CO)_3CH_2C_6H_6$ with tertiary phosphines in toluene at 30 °C.[87]

L	10^6 k ($L\ mol^{-1}s^{-1}$)	ν(CO)[a] (cm^{-1})
PMe_2Ph	19.3	2065.3
PEt_3	19.2	2061.7
$PMePh_2$	9.9	2067.0
PPh_3	4.3	2068.9
$P(i\text{-}Bu)_3$	3.4	2059.7
$P(t\text{-}Bu)Ph_2$	1.9	2064.7

[a] ν(CO) ≡ electronic parameter.

Rate studies were done by Wax and Bergman[78] on the carbonyl insertion reaction of $CpMo(CO)_3CH_3$ in the presence of the nucleophile diphenylmethylphosphine (equation I-21). By using a series of α-methyl-tetrahydrofurans as solvents, they have found that the rates of alkyl migration were drastically influenced by the donicity of the solvent used.

$$CpMo(CO)_3CH_3 + PPh_2Me \rightarrow CpMo(PPh_2Me)(CO)_2(COCH_3) \qquad \text{...I-21}$$

Their results[78] (order of reactivity for k_1: THF > 2-MeTHF >> 2,5-Me_2THF) suggest the direct attack of donor solvent at the metal centre as the alkyl migration is occurring.

1.8 Electrochemical behaviour of some diiron systems.

Interest in diiron cyclopentadienyl complexes[97,102-115] of conjugated systems has been specifically directed at the possibility of interaction between the iron centres. Extensive molecular orbital calculations and spectroscopic studies[110-112] suggest that the metals should strongly interact in the case of a delocalized bridging ligand but should be independent in the case of a non-conjugated system.

The extent of this interaction would thus be indicated by the difference in reduction potentials of the two metal centres.[103,107-109,113] *Cyclic voltammetry is therefore the ideal tool to asses the extent of communication between the two metals.* Electrochemical studies of the mono- (22) and diiron (23) cyclopentadienyl complexes of thianthrene (TH) in acetonitrile were compared by Bligh and co-workers.[103]

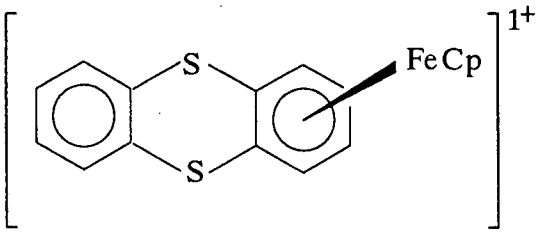

(22)

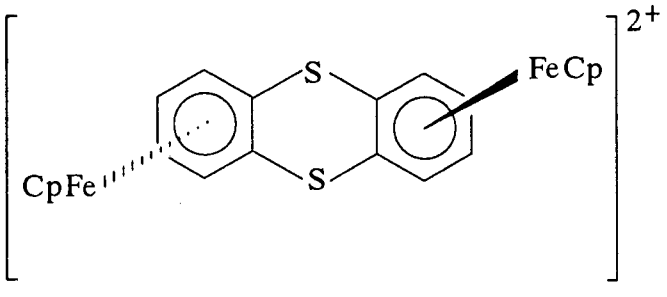

(23)

The cyclic voltammetry of (22) indicates a reversible one-electron reduction in CH_2Cl_2 (E = -0.92 V vs NHE, υ = 200 mV s^{-1}) which becomes irreversible in acetonitrile. The EC mechanism followed in the co-ordinating solvent was also shown to produce ferrocene, benzene and zerovalent iron.

The diiron complex (23) shows under similar conditions, two irreversible reductions in acetonitrile (Ep_1 = -0.81 V, Ep_2 = -1.20 V vs NHE, υ = 50 mV s^{-1}) which become reversible at a scan rate of 20 V s^{-1}.

The mechanism proposed for the heterogeneous charge transfer process is a stepwise reduction of the two metal centres followed by a breakdown of the complex, as a result of solvent interaction with (24) (Scheme I-10)

$$[TH(Fe^{II}Cp)_2]^{2+} + e^- \rightleftharpoons [TH(Fe^{I}Cp)Fe^{II}Cp]^+$$

$$[TH(Fe^{I}Cp)Fe^{II}Cp]^+ + e^- \rightleftharpoons TH(Fe^{I}Cp)_2$$

(24)

SCHEME I-10

The comparative cyclic voltammogram studies of diiron complexes of phenothiazine, diphenylene dioxide and 9,10-dihydroanthracene were studied in acetonitrile (Table I-6). These complexes, which are all anthracene derivatives, should have nearly equal iron-iron distances.

It has been shown[103] that the peak separation of the reductions of two completely non-interacting metals are caused by probability factors only and would in general have a value of $Ep_1 - Ep_2$ = 35.6 mV. In such cases, the resulting voltammogram would be identical to a one-electron reduction wave.

Table I-6 Peak separations for some diiron complexes[a].

Ligand	ΔE/ mV
thianthrene	180
phenothiazine	125
diphenyl dioxide	219
9, 10-dihydroanthracene	125

[a]*Taken from reference 103.*

The diiron complexes of those ligands listed in Table I-6 have $\Delta E \geq 100$ mV, which implies interaction between the two Fe atoms in each case. The reduction potential of the $Fe^{II}Cp$ moiety depends on the charge of the other Fe atom. Also, this interaction is proposed[103] to occur through space or via delocalization through the ligand.

Compounds of the type $[(CpFe)_2(\eta^6\text{-cyclophane})]^{2+}$ **(25)** - **(28)** were shown[104] to undergo two one-electron reductions in acetone (υ = 0.20 V s^{-1}). Although the electrochemistry of these bis(iron) complexes was not always reproducible, the separations of the reduction peaks (Table I-7) were found to be dependent on the solvent, the supporting electrolyte and the cyclophane.

The reduction process is represented by an EE mechanism and describes the sequential reductions of each iron:

$$Fe^{II}Fe^{II} + e^- \rightleftharpoons Fe^{II}Fe^{I} + e^- \rightleftharpoons Fe^{I}Fe^{I}$$

Table I-7 Reductive properties for complexes of the type $[(CpFe)_2(\eta^6\text{-cyclophane})]^{2+}$[a]

Compound	Ep_1/V	Ep_2/V	$\Delta Ep/mV$
25	-1.18	-1.32	140
26	-1.24	-1.40	160
27	-1.16	-1.37	210
28	-1.28	-1.42	140

[a] *Taken from reference 104.*

Similar reduction processes were found[105,106] with $[(CpFe)_2(arene)]^{2+}$ complexes in which each CpFe fragment is bonded to a different centre of the polyaromatic ligands. The measure of interaction between the two iron centres was related to the peak separation between the first and second reductions: a greater interaction will give rise to a greater potential separation.

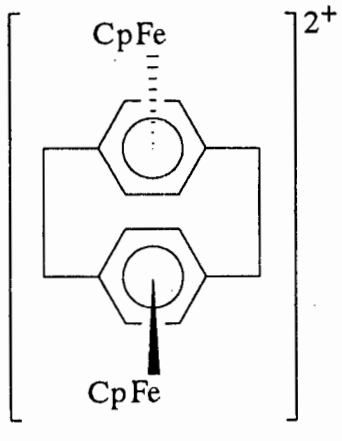

(25)

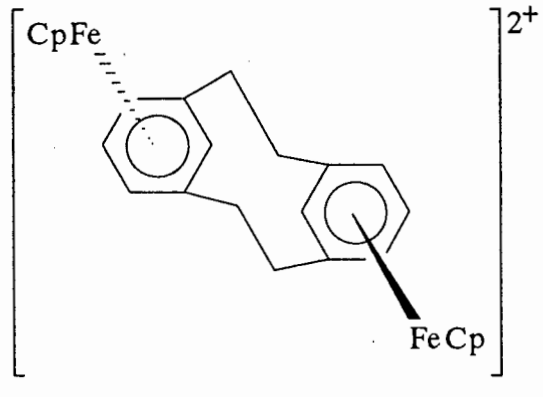

(26)

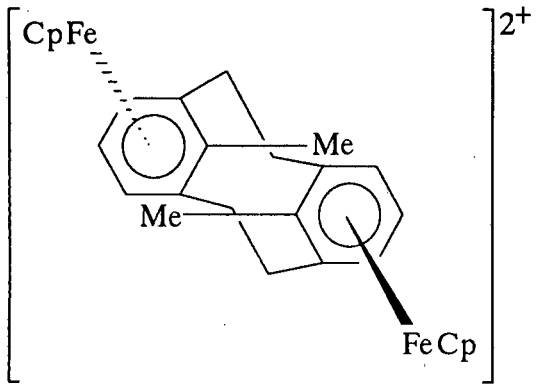

(27)

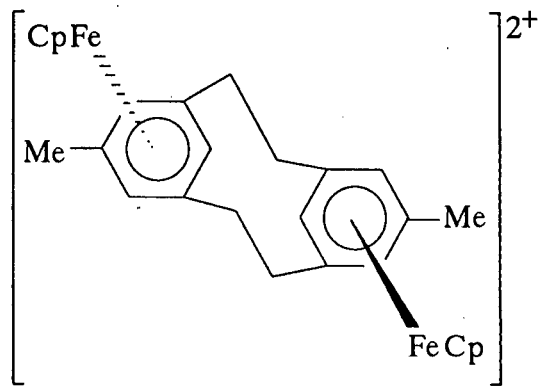

(28)

The electrochemistry of some binuclear iron π-complexes (29), (30)[107] and fused aromatic (31)[109] ligands has also been reported.

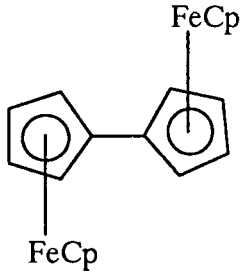

(29)

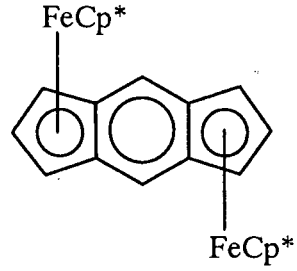

(30)

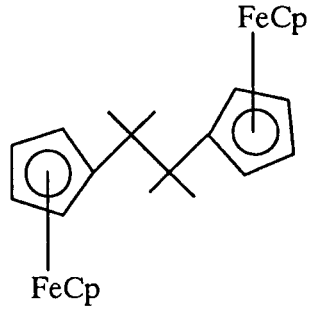

(31)

Two reversible oxidation waves were observed for these compounds which correspond to two successive one-electron oxidations. The magnitude of the separation of these peaks, ΔE (Table I-8), provides a measure of the transmission of charge between the ferrocene-like units.

Table I-8. Difference in oxidation potentials[a] (ΔE) for ferrocenyl type compounds

Compound	ΔE/mV	Reference
29	340	107
30	820	107
31	40	109

[a] *Obtained in dichloromethane, scan rate = 100 mV s^{-1}*

The saturated hydrocarbon-bridged diferrocenes **(29)**, **(31)** were found to be considerably poorer than the fused π-conjugated compound **(30)** in their effectiveness at delocalizing charge. The considerably small ΔE value obtained for **(31)** would suggest the total absence of conjugation between the two metal centres. For binuclear iron(II) compounds, a separation between the first and second oxidation peaks of approximately 1 V manifests charge delocalization.[113]

Objectives of Research

We aim to investigate the electrochemical behaviour of $CpFe(CO)_2(CH_2)_nMo(CO)_3Cp$ in acetonitrile and dichloromethane solutions. These investigations will be done using cyclic voltammetry. This will enable us to gauge how and to what extent the two metals influence each other and hence whether communication exists between them.

Multinuclear organometallic complexes, in general, exhibit complex electrochemical behaviour. Thus it becomes necessary to first investigate the electrochemical behaviour of the mononuclear alkyl complexes of molybdenum (MpR) and that of iron (FpR).

The electrochemistry of some iron methyl complexes has been reported extensively. It is known that the electrochemical oxidation of these complexes in acetonitrile enhances the rate of the subsequent alkyl migration reaction by a factor of 10^6. We were interested in how the oxidation potentials of FpR are affected by changing the length of the R-group. Moreover, whether the electrochemical characteristics of the FpR remain intact in the heterobimetallic complexes $CpFe(CO)_2(CH_2)_nMo(CO)_3Cp$, since this will be indicative of the electrochemical communication between the metal centres.

CHAPTER 2

Results and discussion

2.1 Electrochemistry of $CpFe(CO)_2(CH_2)_nCH_3$

In the present study, the electrochemical oxidation of compounds of the type $CpFe(CO)_2(CH_2)_nCH_3$ (n = 0 to 11) was studied in non- aqueous solvents. It was found that the oxidation process occurs at onset potentials of about 0.8 V (*vs.* Ag/AgCl) and higher. The oxidation process (wave I, Figure 2.1) for these compounds was found to be irreversible at 100 mV s^{-1} in acetonitrile solutions. The peak potentials (Table II-1) were collected from the respective cyclic voltammograms scanned between 0.0 V and 1.1 V, initiated at 0.2 V (zero current potential) initiated in the positive direction.

The oxidation potentials for these complexes may serve as a measure of the relative electron density around the metal centre. Complexes having alkyl groups with stronger σ-donor capacities should enhance the electron density and may therefore ease the oxidation process, thereby shifting the oxidation potential to less anodic values.

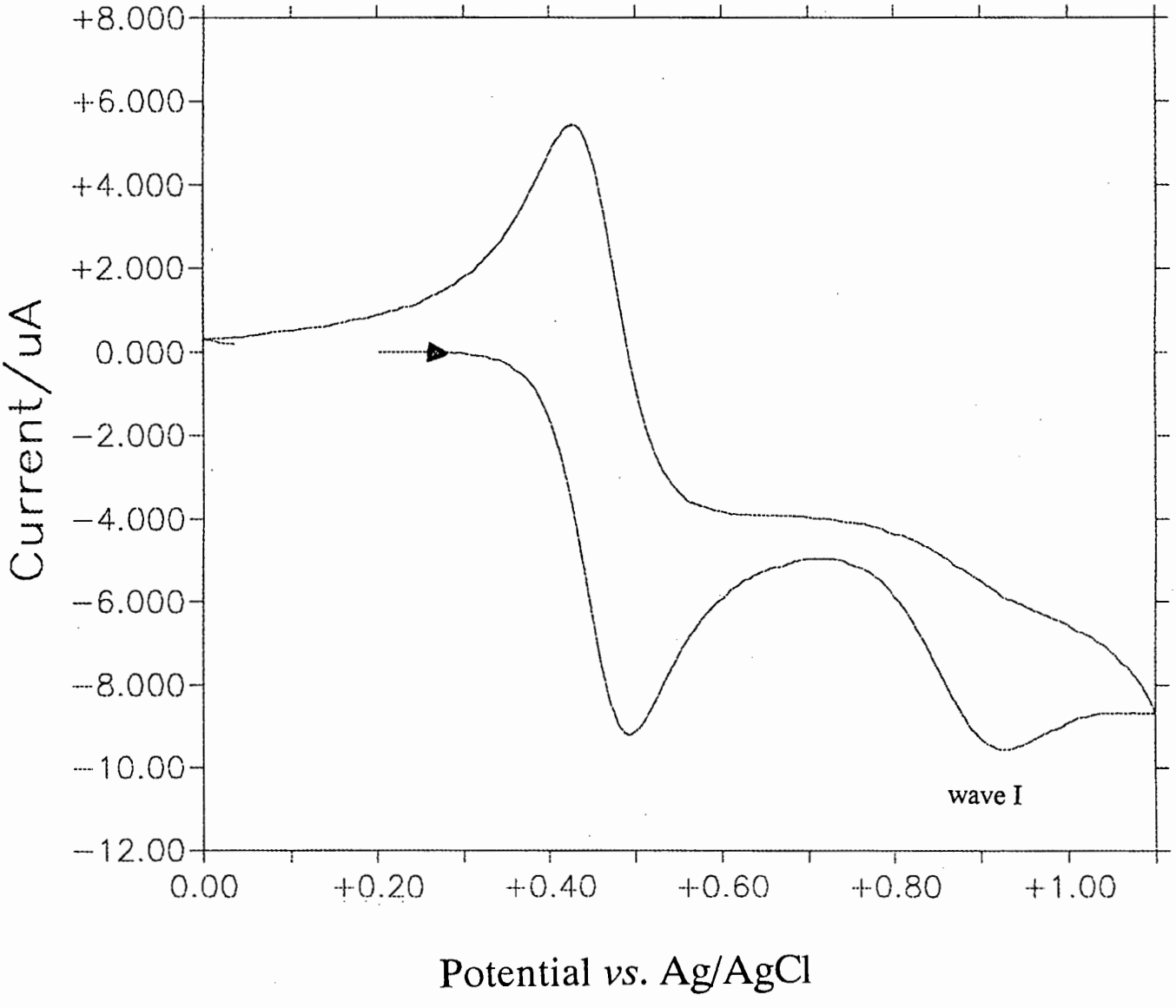

Figure 2.1 Cyclovoltammogram of 8.9×10^{-4} M $CpFe(CO)_2(CH_2)_5CH_3$ in acetonitrile/0.1M $TBABF_4$, scan rate 100 mV s^{-1}. The scan was initiated in the positive direction. The couple on the left is that of Fc/Fc^+.

Table II-1. Oxidation potentials of $CpFe(CO)_2(CH_2)_nCH_3$ in acetonitrile.

n	Concentration/ mole l^{-1}	Wave I E_{pa} / V[a]
0	9.9×10^{-2}	1,004
1	1.4×10^{-3}	0.904
2	1.2×10^{-3}	1.025
3	9.9×10^{-2}	0.954
4	8.7×10^{-2}	0.984
5	9.2×10^{-2}	0.924
6	9.7×10^{-2}	0.921
7	9.6×10^{-2}	0.920
8	9.2×10^{-2}	0.921
9	1.1×10^{-3}	0.928
10	9.8×10^{-2}	0.968
11	1.1×10^{-3}	0.918

[a] *Versus Ag/AgCl, 0.1 M $TBABF_4$.*

No clear correlation was found between the oxidation potential and the length of alkyl group (n-value). In addition, ^{13}C NMR data[96] for the series of iron alkyl compounds with R = *n*-C_6H_{13} to *n*-$C_{12}H_{25}$ showed no appreciable variation in the chemical shift of the resonances for the α-carbon of the alkyl ligand.

Table II-2 lists the Tolman's χ_i- values[66] (see p. 18), which is a quantification of σ-donor capacities, for a few R-groups. These values predict the iron methyl compound to have a slightly higher anodic potential and that, that of the ethyl and butyl analogues not to differ much.

Table II-2 Tolman's χ_i -values for some substituents.[a]

R-group	χ_i
CH_3	2.6
CH_2CH_3	1.8
$CH_2\,CH_2\,CH_2\,CH_3$	1.4
CF_3	19.6

[a] Taken from reference 66.

These values (Table II-2) show that the increasing chain length should not cause a remarkable increase in the electron density on the metal in our complexes. One would therefore also expect χ_i values not to increase as a function of the increase in chain length, but in fact to hardly differ from the above values. Our experimentally obtained E_{pa}- values (Table II-1) appear to indicate this.

Electrochemical studies[59-61,90-95] that have been carried out on similar systems (including $CpFe(CO)_2Me$) have shown that the mechanism followed after electrochemical oxidation in acetonitrile is that as outlined in Scheme 2-1.

We have run several cyclic voltammograms on our $CpFe(CO)_2R$ complexes which could all be interpreted by Scheme 2-1.

Electrolysis at potentials slightly more anodic than the corresponding oxidation potential gives, on the back scan, a growth in height of wave II (Figure 2.2(b)). Also, scanning from zero current potential in the positive direction with E_λ smaller than the onset potential of wave I, leads to, upon scan reversal, the disappearance of wave II.

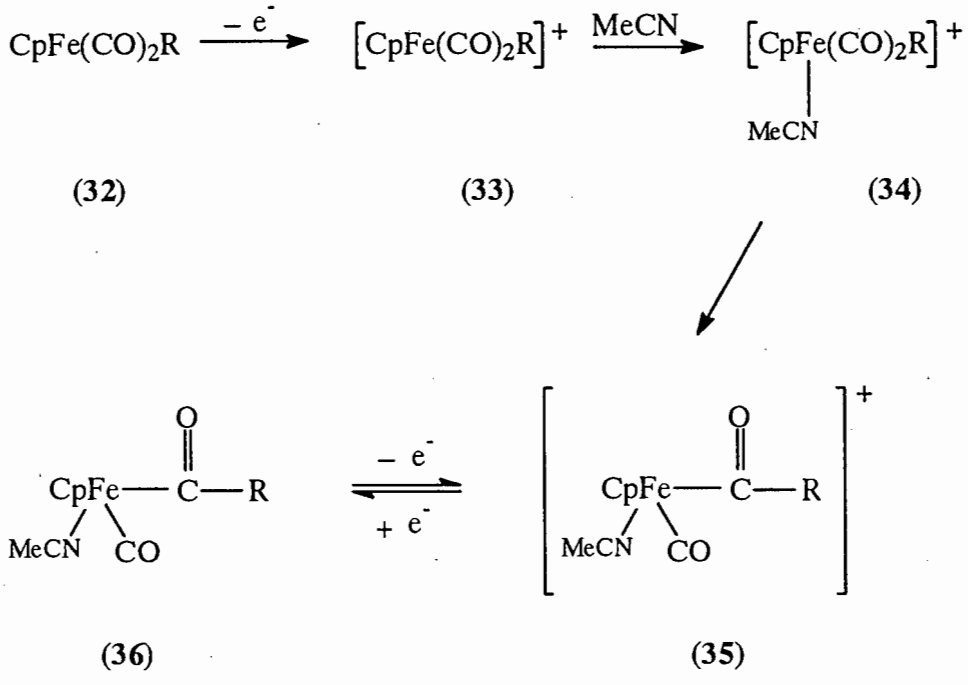

SCHEME 2-1

These observations thus clearly demonstrate the dependence of wave II on the oxidised species. The cation (33), is known[91-95] to undergo alkyl migration at a very fast rate, and the reduction thereof was unobservable at scan rates up to 10^5 mV s^{-1}. Hence, the reduction that is observed (wave II) is that of (35) → (36). The oxidation process of these iron alkyl compounds could therefore be described as following an ECE mechanism.

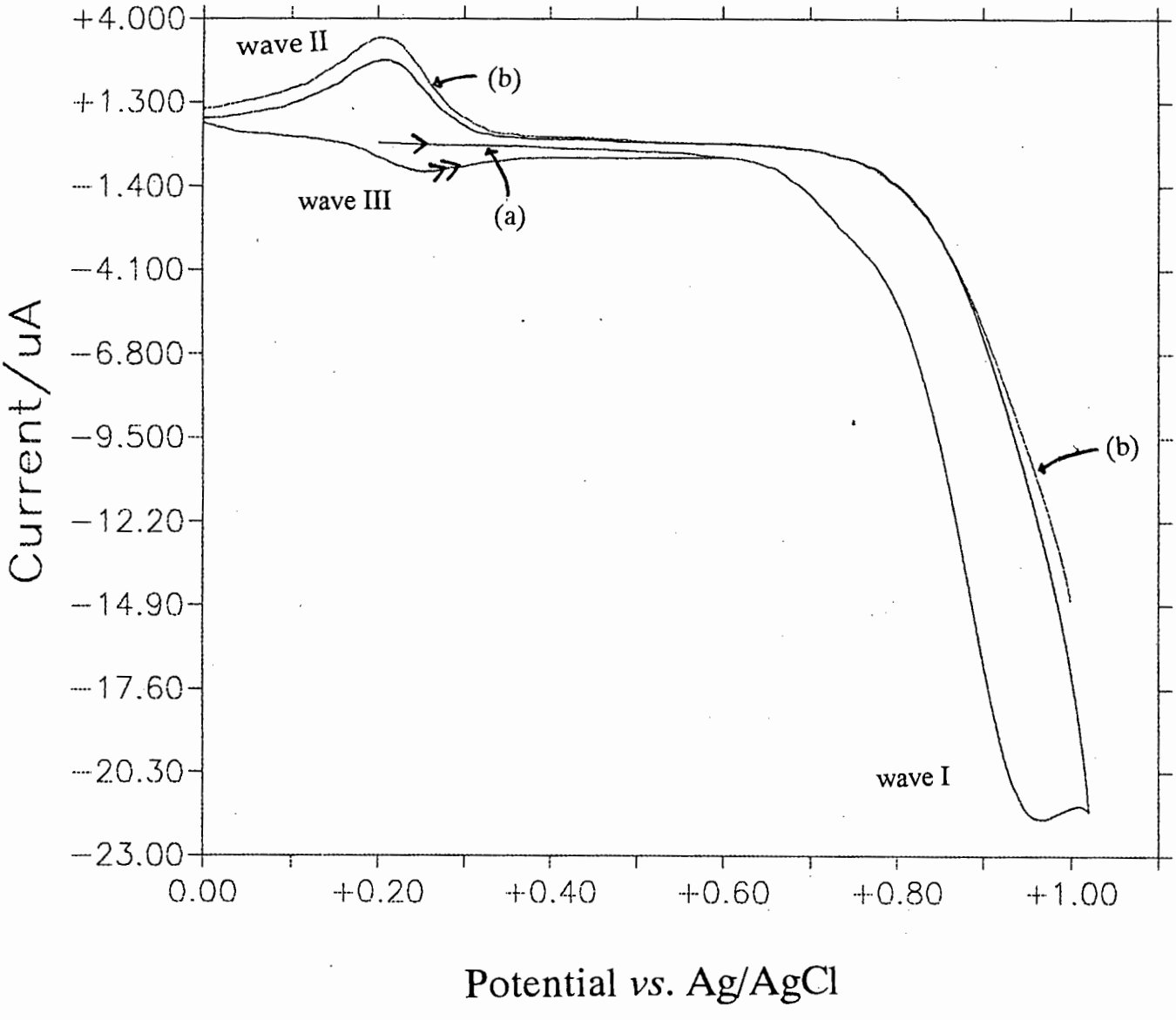

Figure 2.2 *(a)* Cyclic voltammogram of 1.4×10^{-3} M $CpFe(CO)_2(CH_2)_3CH_3$ in acetonitrile/0.1 M $TBABF_4$. *(b)* Growth in peak II is observed after electrolysis at slightly more anodic potentials than E_{pa}.

Completing the cycle, and scanning beyond the starting potential produces an oxidation wave III which was absent during the first scan (Figure 2.3). Furthermore, wave III was found to be coupled to wave II and represents the redox reaction (35) $\rightleftharpoons$ (36) in Scheme 1. Table II-3 lists the electrochemical data pertaining to waves II and III for $CpFe(CO)_2(CH_2)_nCH_3$. These data were collected from the respective cyclic voltammograms scanned between 0.0 V and 1.1 V, initiated at 0.2 V (zero current potential) in the positive direction.

Table II-3. Cyclic voltammetry data for waves II and III of $CpFe(CO)_2(CH_2)_nCH_3$.

n	Wave II E_{pc} / V[a]	Wave III E_{pa} / V[a]	ΔE / mV[b]	i_{pa}/i_{pc}
0	0.241	0.272	31	0.164
1	0.211	0.257	46	0.154
2	0.197	0.238	41	0.186
3	0.199	0.250	51	0.201
4	0.200	0.245	45	0.393
5	0.219	0.264	45	0.340
6	0.203	0.250	47	0.505
7	0.201	0.257	56	0.637
8	0.189	0.238	49	0.496
9	0.207	0.241	33	0.335
10	0.210	0.263	53	0.450
11	0.207	0.248	42	0.170

[a]Versus Ag/AgCl, 0.1 M $TBATBF_4$, scan rate 100 mV s^{-1}. [b]$\Delta E = E_{pa} - E_{pc}$. Concentrations are the same as in Table II-1.

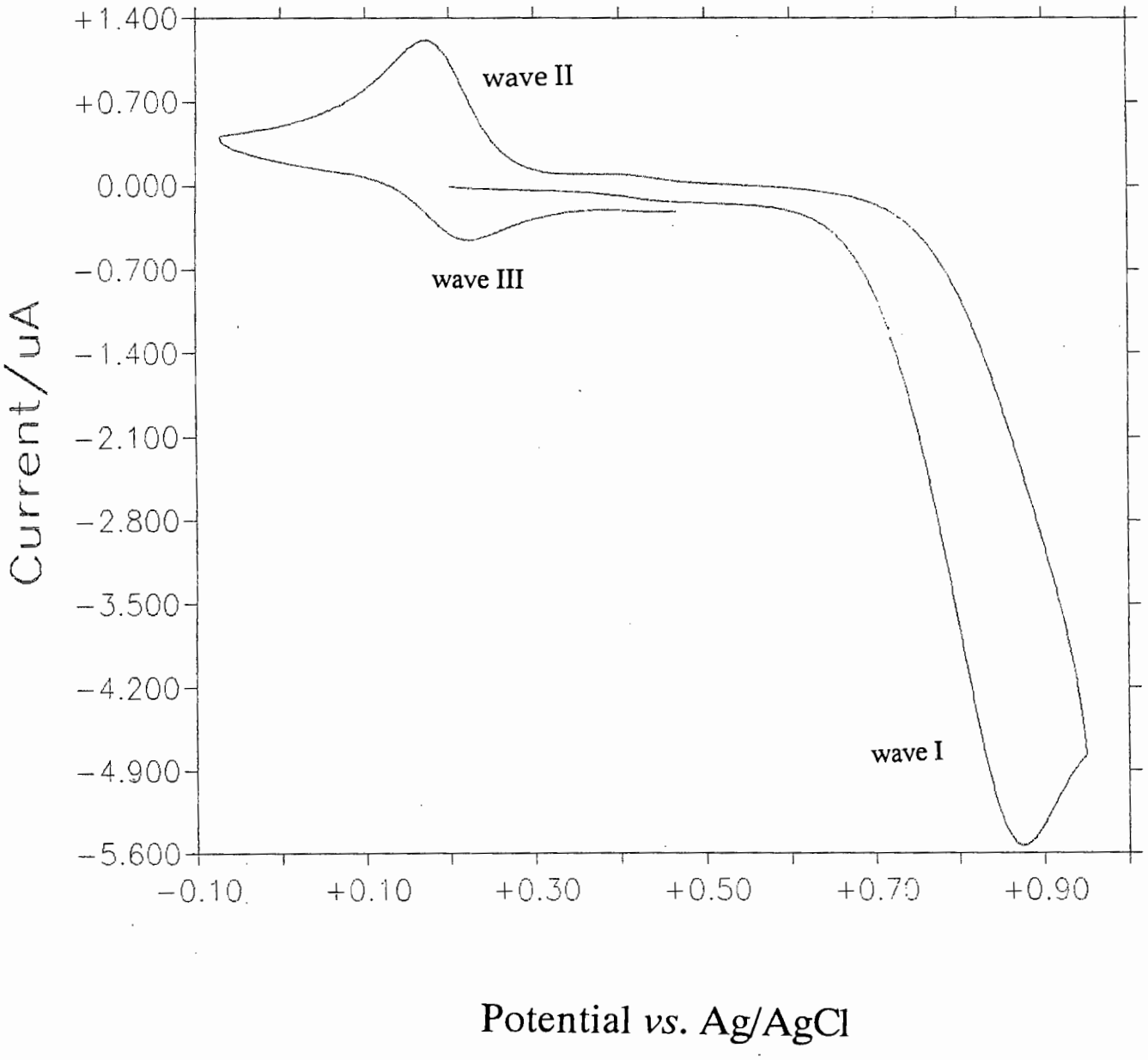

Figure 2.3 Cyclic voltammogram of 5.1×10^{-4} M $CpFe(CO)_2CH_2CH_3$ in acetonitrile/0.1M $TBABF_4$. Anodic wave III appears only after wave II had been scanned.

It has been proposed[92] that the acyl species (36) can revert back to the starting complex (1) via decarbonylation. If this so, then not all of (36), that is produced during wave II , is available (and thus electroactive) for oxidation during wave III. The ratio of the peak currents i_{pa}/i_{pc} (Table II-3) was found to be less than unity for all the iron alkyl compounds, indicating a quasi-reversible couple. Thus, an ECE mechanism is followed during this redox couple and this is reflected in the quasi-reversibility. Voltammograms for $CpFe(CO)_2R$ (Figures 2.4 to 2.8) obtained in dichloromethane and/or acetonitrile support the mechanism as outlined in Scheme 2-1:

(i) Changing the solvent from CH_3CN to the non-coordinating solvent dichloromethane would prohibit the formation of the solvated 19e$^-$ cation. The resulting CV should thus show the absence of the waves II and III, as was observed, see Figure 2.4. The anodic peak potentials for the iron alkyl compounds are listed in Table II-4. These values were collected from the respective CV's scanned between 0.0 V and 1.2 V, initiated at 0.2 V (zero current potential) in the positive direction.

(ii) The addition of small amounts of acetonitrile to the above solution should make the formation of (35) possible and lead to the growth in the cathodic peak for the reduction of (35) (Figure 2.5).

Table II-4. Oxidation potentials of $CpFe(CO)_2(CH_2)_nCH_3$ in dichloromethane.

n	M/mole l^{-1}	Wave I E_{pa} /V[a]
0	1.7×10^{-3}	1.184
1	1.2×10^{-3}	1.181
2	5.5×10^{-2}	1.175
3	9.1×10^{-2}	1.129
4	8.1×10^{-2}	1.073
5	9.7×10^{-2}	1.159
6	8.7×10^{-2}	1.111
7	1.4×10^{-3}	1.148
8	9.6×10^{-2}	1.190
9	1.5×10^{-3}	1.194
10	9.1×10^{-2}	1.192
11	1.0×10^{-3}	1.162

[a] *Peak values, vs. Ag/AgCl*

(iii) Cycling the voltammograms over the quasi-reversible couple after the initial oxidation wave (E_{pa}) had been scanned, shows a remarkable drop in current of the waves of this couple with time (Figure 2.6). This scan format essentially prevents the further production of (33) (and therefore also (35)), after wave I had been scanned. The resulting voltammograms are interpreted as follows:

(a) Depending on the scan direction over the couple, the working electrode is at any stage surrounded by (35) and/or (36). Since this couple was found to be quasi-reversible, the concentration of the electroactive species will steadily diminish around the working electrode with time.

(b) It has been suggested[92-93] that (36) reverts to (32) via decarbonylation. The drop in current during each successive scan over waves II and III would indeed give us some insight into the relative reaction rate of this process, since it would be directly related to the amount of the iron acyl compound (36) that is converted to the parent molecule (32).

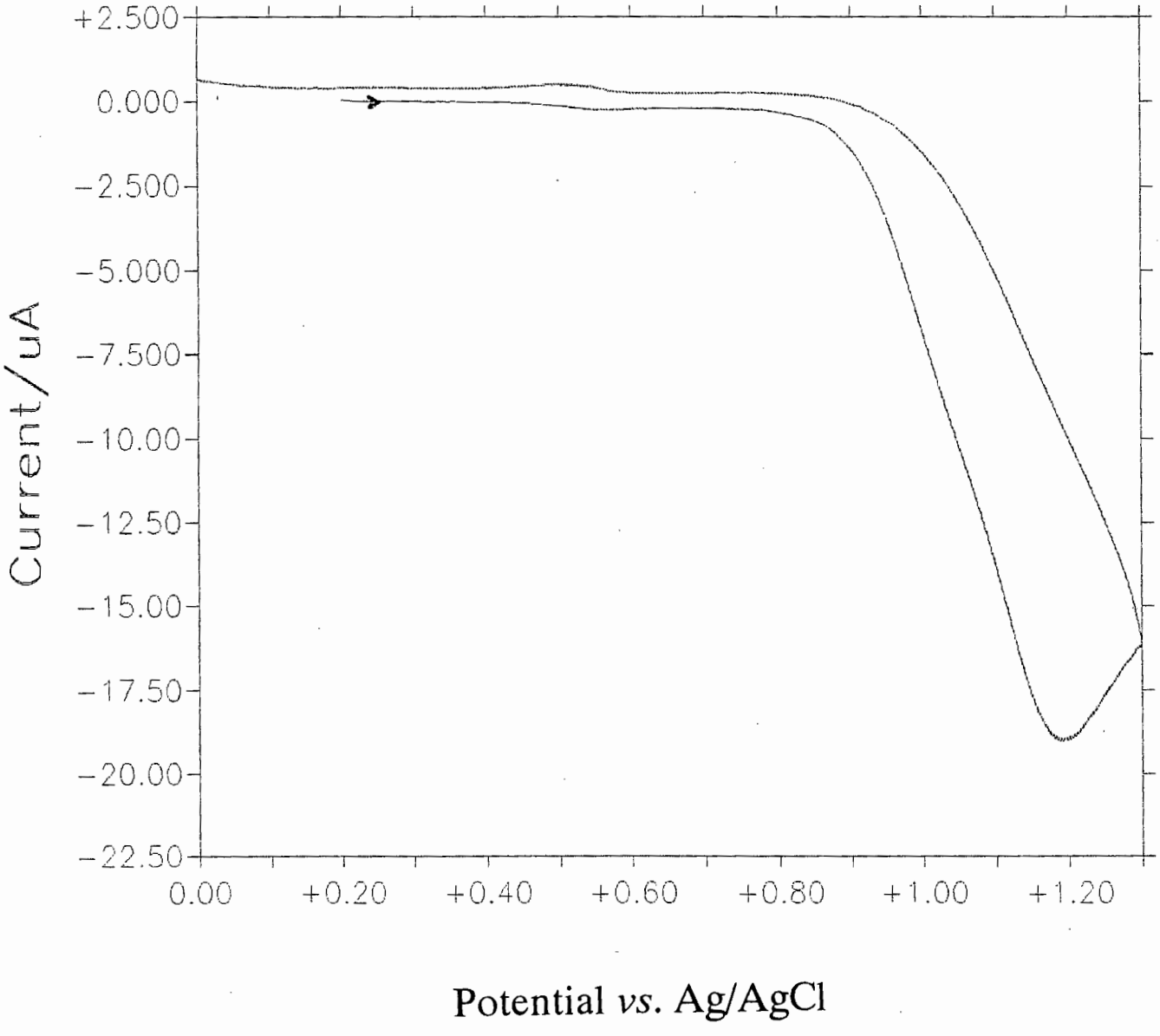

Figure 2.4 Cyclic voltammogram of 1.2×10^{-3} M $CpFe(CO)_2CH_2CH_3$ in dichloromethane/0.1M $TBAFB_4$ *versus* Ag/AgCl. Note the absence of the couple. The small peaks at *ca.* 0.5 V is due to impurities in the solvent.

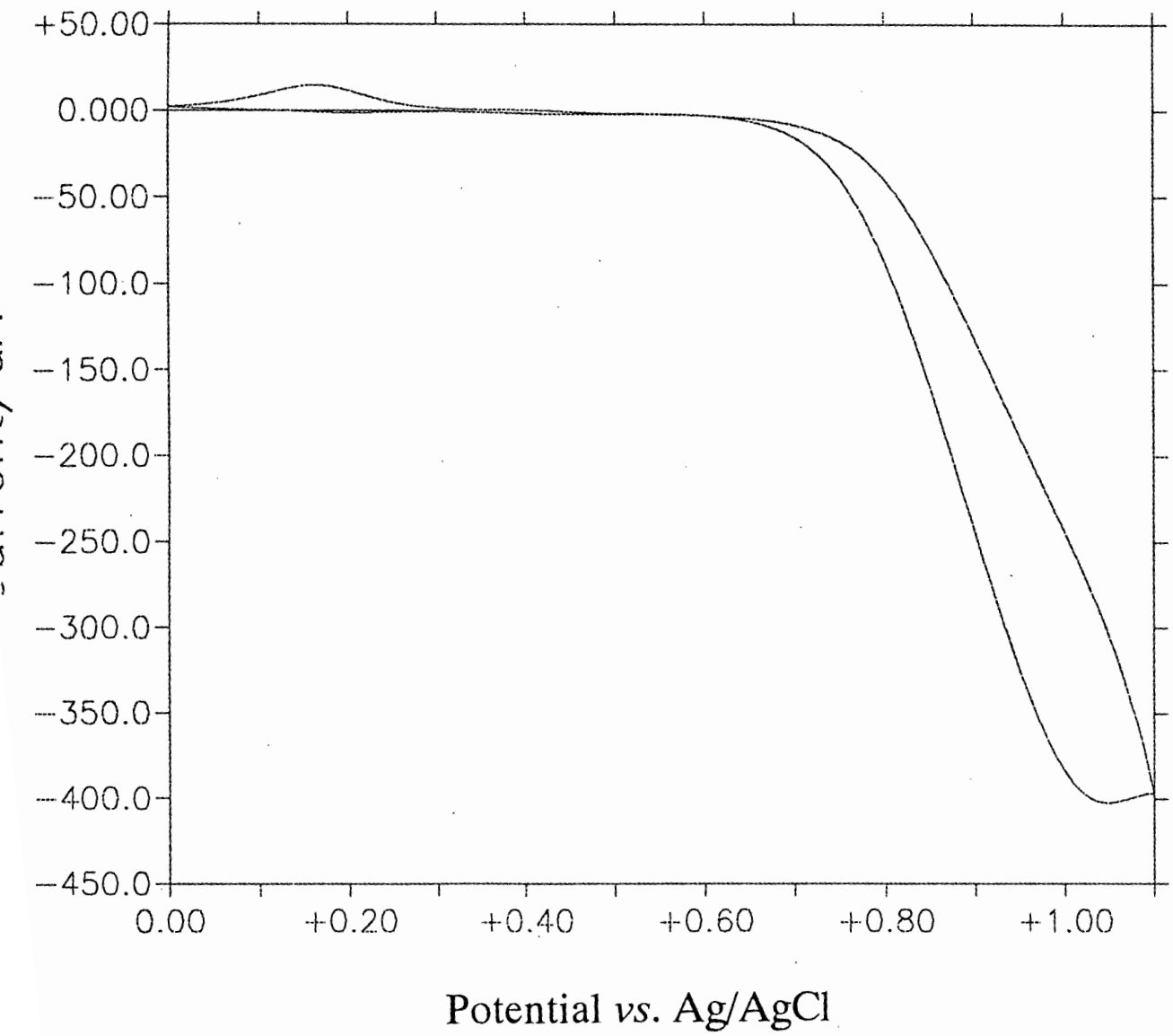

ıre 2.5 Cyclic voltammogram of 1.1×10^{-3} M $CpFe(CO)_2(CH_2)_4CH_3$ in 30% acetonitrile in dichloromethane/0.1M $TBABF_4$, *versus* Ag/AgCl, scan rate = 100 mV s^{-1}.

The ratio of currents of waves II and III was determined for a few iron alkyl compounds (Table II-3). The values of the peak currents were taken from voltammograms scanned between 1.1 V and 0.0 V, initiated at 0.2 V (zero current potential) in the positive direction. The magnitudes of the currents of these waves are directly proportional to the concentration of the corresponding electroactive species, according to the Randles-Sevcik equation. It should be pointed out however, that although the time elapsed from the moment the peak potential of wave II had been scanned to that of wave III is not the same for these compounds, the calculated ratios should be considered as being an approximation to the relative rates of decarbonylation.

The data (Table II-3) essentially suggest a faster rates of decarbonylation for the short chain alkyl complexes than for the longer chain iron alkyls. These results are in contrast with that found by Moss and Andersen[116] for the thermal decarbonylation of acylmanganese pentacarbonyl compounds $[Mn(COR)(CO)_5]$ ($R = CH_3$ to n-$C_{17}H_{35}$).

(c) The amount of (32) which is oxidised during wave I is not reproduced at the end of any scan, but is in fact converted to (35) and (36). If a second cycle is scanned *immediately after the first,* a decrease in current for wave I should then be observed (Figure 2.7).

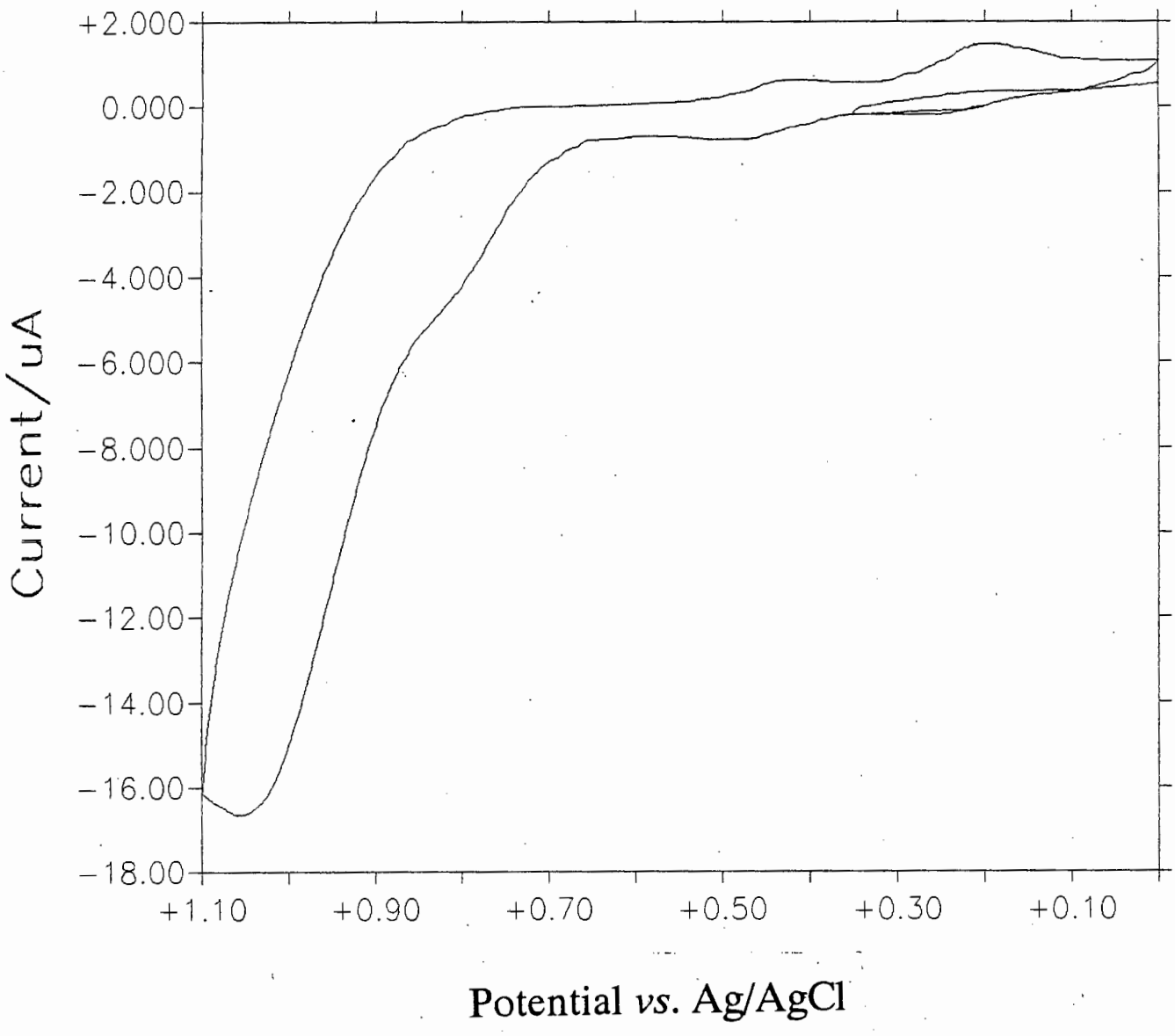

Figure 2.6 Cyclic voltammogram of 1 X 10^{-3} M $CpFe(CO)_2(CH_2)_4CH_3$ in acetonitrile/0.1M $TBABF_4$, *versus* Ag/AgCl, scan rate = 100 mV s^{-1}. The scan was initiated at 0.2 V and allowed to cycle over the quasi-reversible couple, waves II and III.

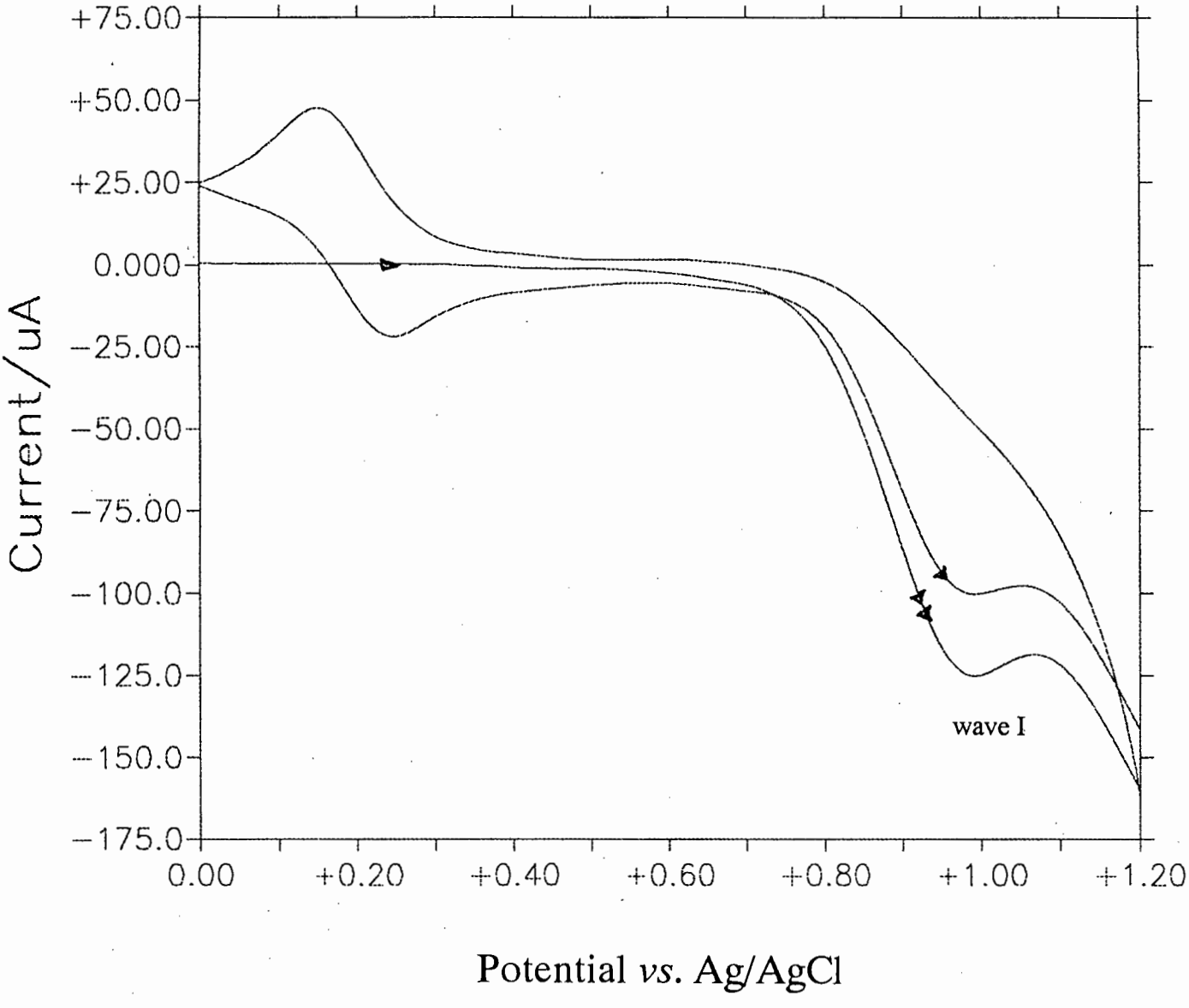

Figure 2.7 Cyclic voltammogram of $CpFe(CO)_2(CH_2)_{11}CH_3$ in acetonitrile/0.1M $TBABF_4$, *versus* Ag/AgCl, scan rate = 600 mV s^{-1}. The scan was initiated at 0.0 V and allowed to cycle over waves I to III.

The addition of triphenylphosphine to a dichloromethane solution of the iron alkyl compound, $CpFe(CO)(CH_2)_2CH_3$ shows the appearance of a new oxidation wave at a more positive potential than the corresponding wave I (Figure 2.7). This is most probably due to the oxidation of the acyl complex formed by the coordination of PPh_3 to the metal before initial oxidation of $CpFe(CO)(CH_2)_2CH_3$ (equation 1):

$$CpFe(CO)(CH_2)_2CH_3 + PPh_3 \rightarrow CpFe(CO)(PPh_3)C(O)(CH_2)_2CH_3 \quad ...(1)$$

The infrared spectrum of the sample above shows the presence of both the acyl function at $\upsilon(CO) = 1609\ cm^{-1}$ of $CpFe(CO)(PPh_3)C(O)(CH_2)_2CH_3$ and the terminal carbonyl stretching frequencies of $CpFe(CO)(CH_2)_2CH_3$.

The consistent appearance of a reduction peak (wave IV) at about -0.30 V (*versus* Ag/AgCl) was observed, after the initial oxidation peak was scanned, for all of the iron-alkyl compounds (Table II-5). Bullock *et al*[97] reported a similar reduction wave for the subsequent behaviour of the dimer $[CpFe(CO)_2]_2$, upon electrochemical oxidation (Scheme 2-2). In dichloromethane the $16e^-$ cation $[CpFe(CO)_2]^+$, showed two reduction waves with increasing amounts of acetonitrile, which was attributed to the reduction of the acetonitrile and aqua complexes.

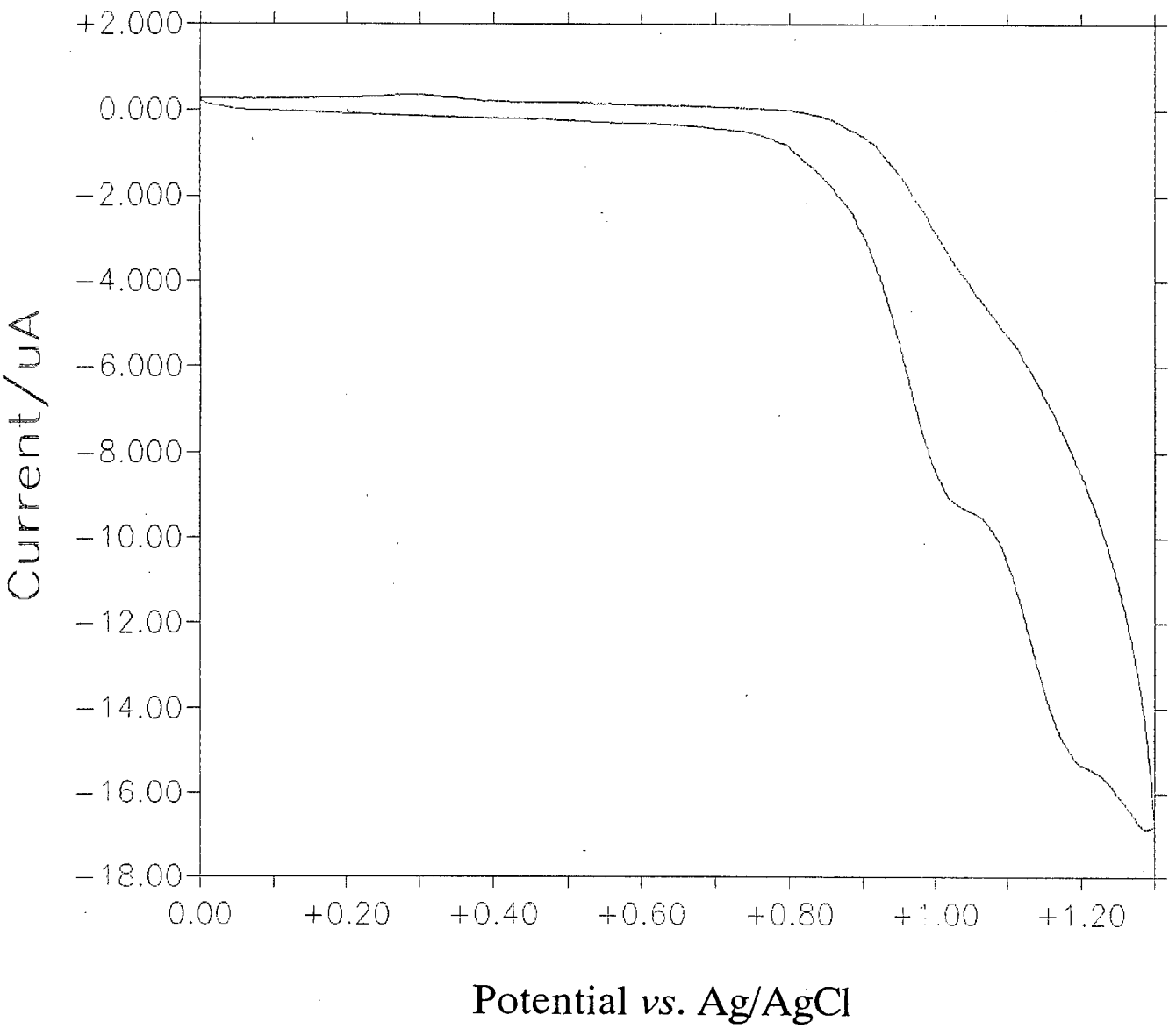

Figure 2.8 Cyclic voltammogram of 9.1×10^{-4} M $CpFe(CO)_2(CH_2)_2CH_3$ in dichloromethane/0.1M $TBAFB_4$, *versus* Ag/AgCl. Addition of PPh_3 results in the appearance of a new anodic wave.

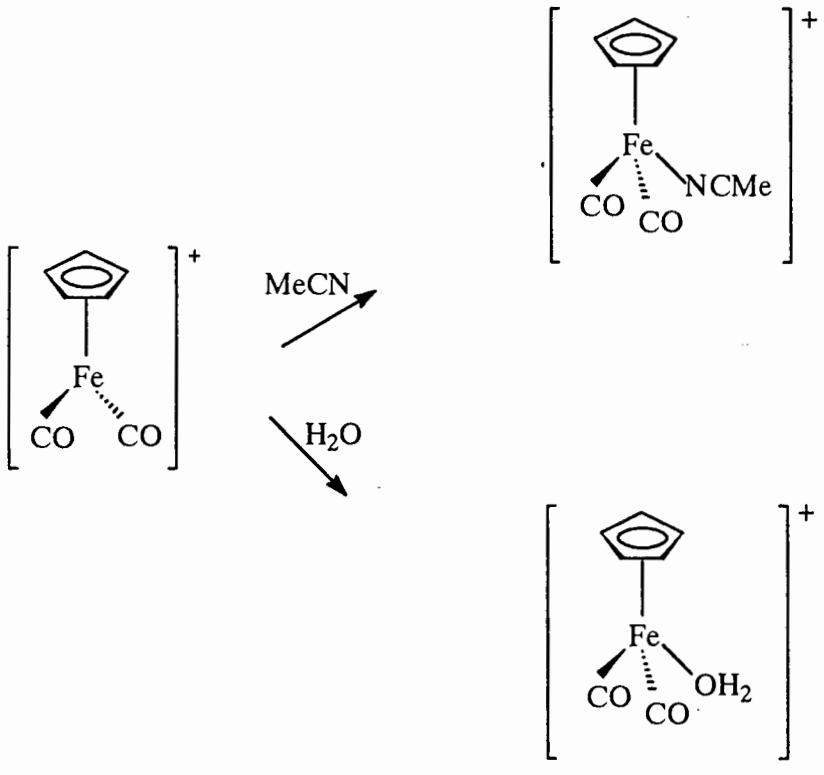

SCHEME 2-2 Mehanism for the formation of $CpFe(CO)(OH_2)$

We have found a growth in the reduction wave when small amounts of water were added to the solution, which supports the formation of $[CpFe(CO)(OH_2)(COR)]^+$[93], most probably due to the presence of adventitious water in our solvent. This wave would thus represent the reduction of this complex:

$$[CpFe(CO)(OH_2)(COR)]^+ + e^- \rightarrow [CpFe(CO)(OH_2)(COR)]$$

Table II-5. Peak potentials of waves IV of $CpFe(CO)_2(CH_2)CH_3$.

n	Wave IV E_{pc} / V[a]
0	-0.284
1	-0.361
2	-0.289
3	-0.303
4	-0.318
5	-0.316
6	-0.297
7	-0.352
8	-0.300
9	-0.282
10	-0.291
11	-0.282

[a] Versus Ag/AgCl, 0.1 $TBABF_4$. Concentrations are similar to that of Table II-1.

In summary, the iron alkyl compounds exhibit different electrochemical behaviour in the two solvents, acetonitrile and dichloromethane. After the initial electrochemical oxidation of FpR in acetonitrile, the solvent coordinates to the metal followed by the alkyl migration reaction. This was not observed when dichloromethane was used as the solvent. In order to get an insight as to how the electrochemical mechanism (especially in acetonitrile) will be affected around the Fe centre in the heterobimetallic complexes $Fp(CH_2)_nMp$, it becomes inevitable to study the electrochemistry of a few molybdenum alkyl compounds.

2.2 The electrochemistry of $CpMo(CO)_3(CH_2)_nCH_3$ (n = 3, 4, 17)

The oxidation of Mp-R (Mp = $CpMo(CO)_3$; R = n-butyl, n-pentyl, n-octadecyl) in acetonitrile is observed as an irreversible anodic wave. Cyclic voltammograms of these compounds produce ill-defined reduction peaks upon scan reversal (Figure 2.8), which grow when electrolysing the solutions at potentials slightly more positive than that of the corresponding oxidation peaks (Table II-4). We have not been able to interpret these reduction peaks.

Table II-6 Oxidation potentials of some molybdenum-alkyl compounds.

n in $CpMo(CO)_3(CH_2)_nCH_3$	E_{ox} (V)[a]
3	1.154
4	1.174
17	1.195

[a] *Peak values, versus Ag/AgCl.*

It has been shown[78] that (19) exists as the acylated species in coordinating solvents. Infrared spectra of our molybdenum alkyl compounds run in acetonitrile however, have shown no absorbance in the acyl stretching frequency region. Thus, the anodic potentials (Table II-6) are associated with the oxidation process of the corresponding molybdenum alkyl compound, and not its acyl analogue.

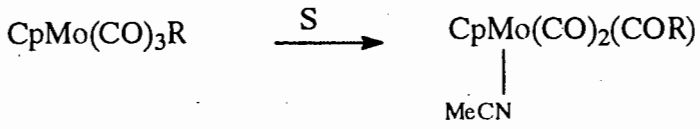

(19)

S = methyl-substituted terahydrofurans

The peak values obtained confirm that the oxidation potentials for $CpMo(CO)_3(CH_2)_nCH_3$ are slightly higher than those for the corresponding iron-alkyl compounds. This information proved to be vital for the interpretation of the elctrochemical behaviour of the hetero-bimetallic compounds of the type $Cp(CO)_2Fe(CH_2)_nMo(CO)_3Cp$ (n = 3 to 6) (Section 2.3) which contain both molybdenum and iron.

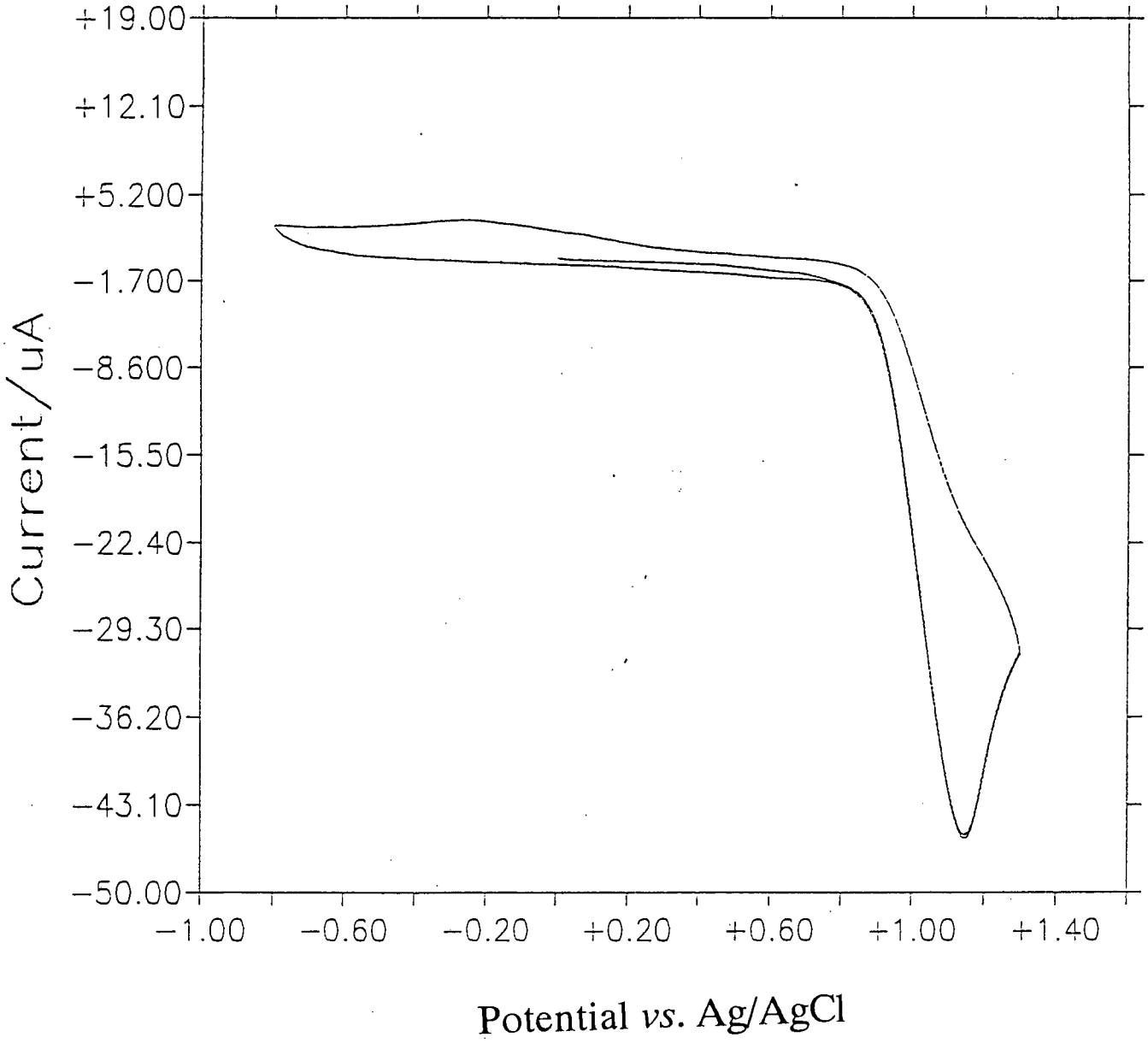

Figure 2.9 Cyclic voltammogram of 1.5×10^{-3} M $CpMo(CO)_3(CH_2)_{17}CH_3$ in acetonitrile/0.1M $TBAFB_4$, *versus* Ag/AgCl, scan rate = 100 mV s^{-1}.

2.3 The electrochemistry of $CpFe(CO)_2(CH_2)_nMo(CO)_3Cp$ (n = 3 to 6)

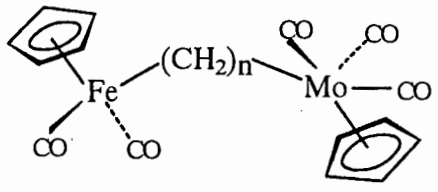

The anodic oxidation of $Cp(CO)_2Fe(CH_2)_nMo(CO)_3Cp$ was investigated in dichloromethane and acetonitrile solutions, at room temperature. Cyclic voltammograms of $Fp(CH_2)_nMp$ (Fp = $CpFe(CO)_2$; Mp = $CpMo(CO)_3$) suggest different electrochemical behaviour in these solvents.

In the coordinating solvent MeCN, the oxidation of $Fp(CH_2)_nMp$ appears to occur as a two-step process (Figure 2.9). When scanning from the rest potential to more positive potentials at 100 mV s^{-1}, two consecutive, irreversible anodic waves (Table II-7) are encountered. These waves are very closely spaced, the first of which is just resolved.

Table II-7 Oxidation peaks for $Cp(CO)_2Fe(CH_2)_nMo(CO)_3Cp$ in acetonitrile.

n	1st oxidation (V)[a]	2nd oxidation (V)[a]	ΔE(V)[b]
3	1.320	1.535	0.215
4	1.322	1.162	0.160
5	1.360	1.585	0.225
6	1.319	1.564	0.245

[a] Peak values, *vs* Ag / AgCl; scan speed, υ = 100 mV s^{-1}; [b] ΔE = 2nd - 1st oxidation potential

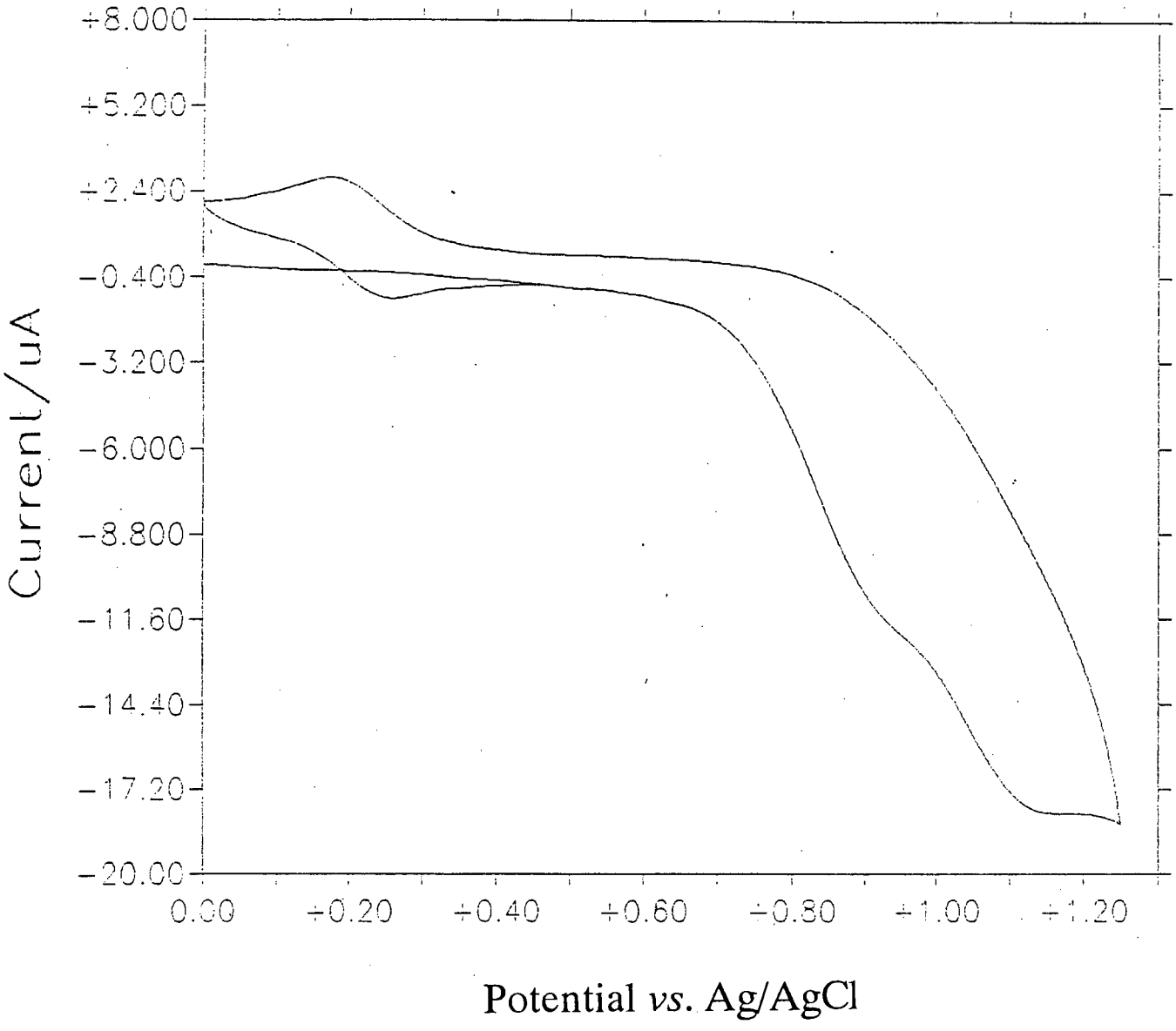

Figure 2.10 Cyclic voltammogram of 8.9×10^{-4} M $Fp(CH_2)_4Mp$ in acetonitrile/0.1M $TBABF_4$, *versus Ag/AgCl.*

On the reverse scan, a quasi-reversible couple is observed. Scans to establish the interdependence of this couple on the oxidation waves were run as follows:

Cyclic voltammograms were initiated from the rest potential up to increasing switching potentials, up to slightly less cathodic than that of the first oxidation peak. (This method of investigation was preferred over electrolysis because we wanted to exclude the second anodic wave in the scans; electrolysis at more positive potentials than that of the first peak value could produce products which are oxidisable at the second peak as a result of the closeness of these two peaks.)

A remarkable increase of the quasi-reversible couple was found with increasing switching potentials (Figures 2.11a - d). This observation clearly indicates the dependence of the couple on the *first oxidation wave.* Cycling the voltammogram over the potential range (including only the couple), show a sharp decrease in current with time (Figure 2.12). Thus, Figures 2.11 and 2.12 show a striking similarity with cyclic voltammograms obtained from the iron alkyl compounds, $CpFe(CO)_2R$ in acetonitrile.

In CH_2Cl_2, however, the oxidation of $Fp(CH_2)_4Mp$ (Table II-8) is represented by one ill defined irreversible wave at Ep = 1,201 V at a scan rate of 100 mV s^{-1} (Figure 2.13). On the return scan no significant reduction peaks were observed up to -1,00V.

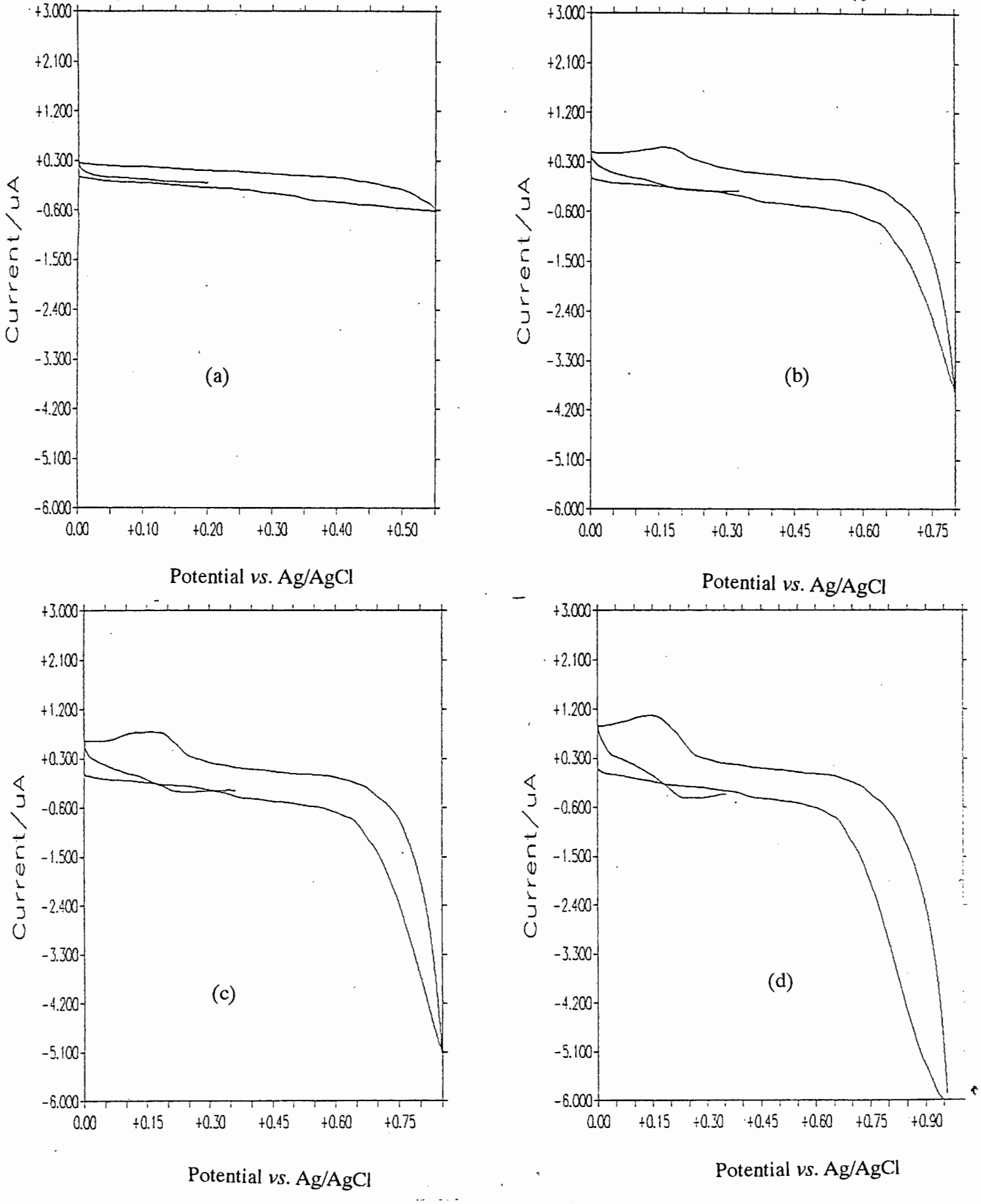

Figure 2.11 Cyclic voltammogram of 1.9×10^{-4} M $Fp(CH_2)_4Mp$ in acetonitrile/0.1M $TBABF_4$ The scans were initiated from 0.0 V (*vs* Ag/AgCl), each time with diffrent E_λ.

Table II-8 Oxidation peaks for $Cp(CO)_2Fe(CH_2)_nMo(CO)_3Cp$ in dichloromethane.

n	1st oxidation (V)[a]
4	1.120
5	1.498
6	1.524

[a] *Peak potentials, versus Ag/AgCl.*

The addition of MeCN (25% by volume) to solutions of $Fp(CH_2)_5Mp$ in CH_2Cl_2 results in the sudden appearance of a quasi-reversible couple. This couple was previously found by us in neat acetonitrile solutions (Figure 2.14).

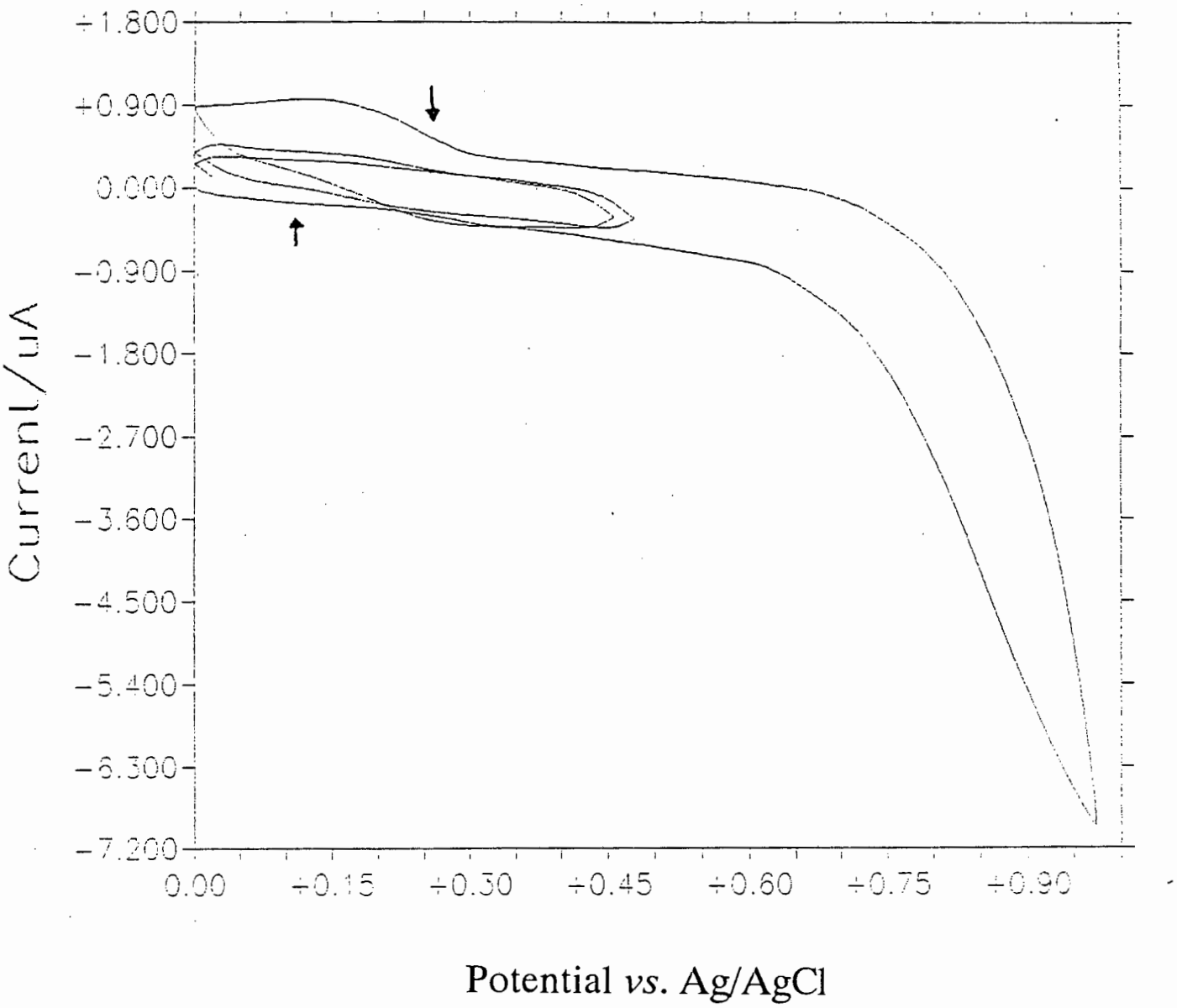

Figure 2.12 Cyclic voltammogram of 1.9×10^{-4} M $Fp(CH_2)_4Mp$ in acetonitrile/0.1M $TBABF_4$. The scans were cycled over the quasi-reversible couple after the first oxidation wave had partially been scanned.

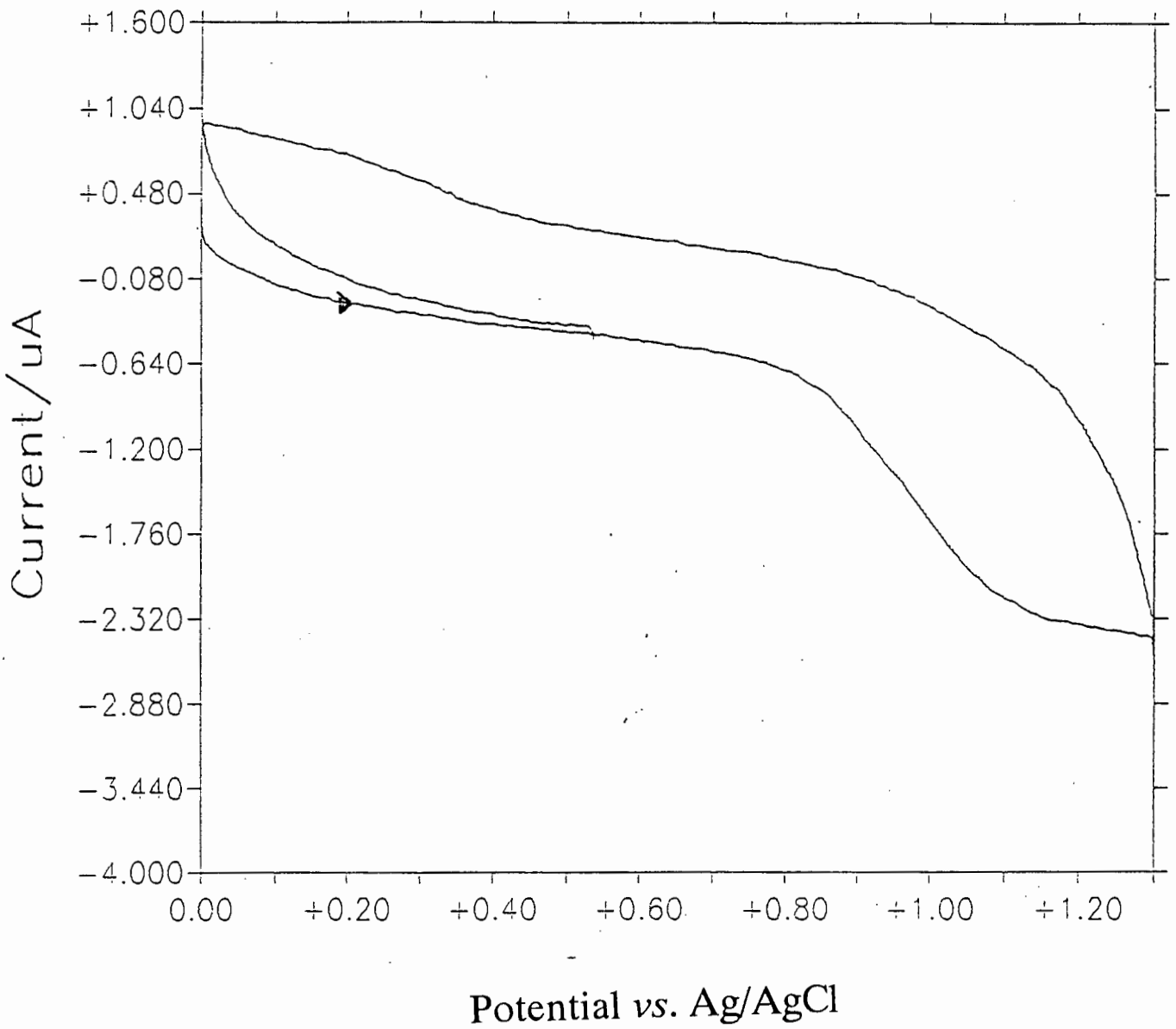

Figure 2.13 Cyclic voltammogram of 1.5×10^{-4} M $Fp(CH_2)_4Mp$ in dichloromethane/0.1M $TBABF_4$.

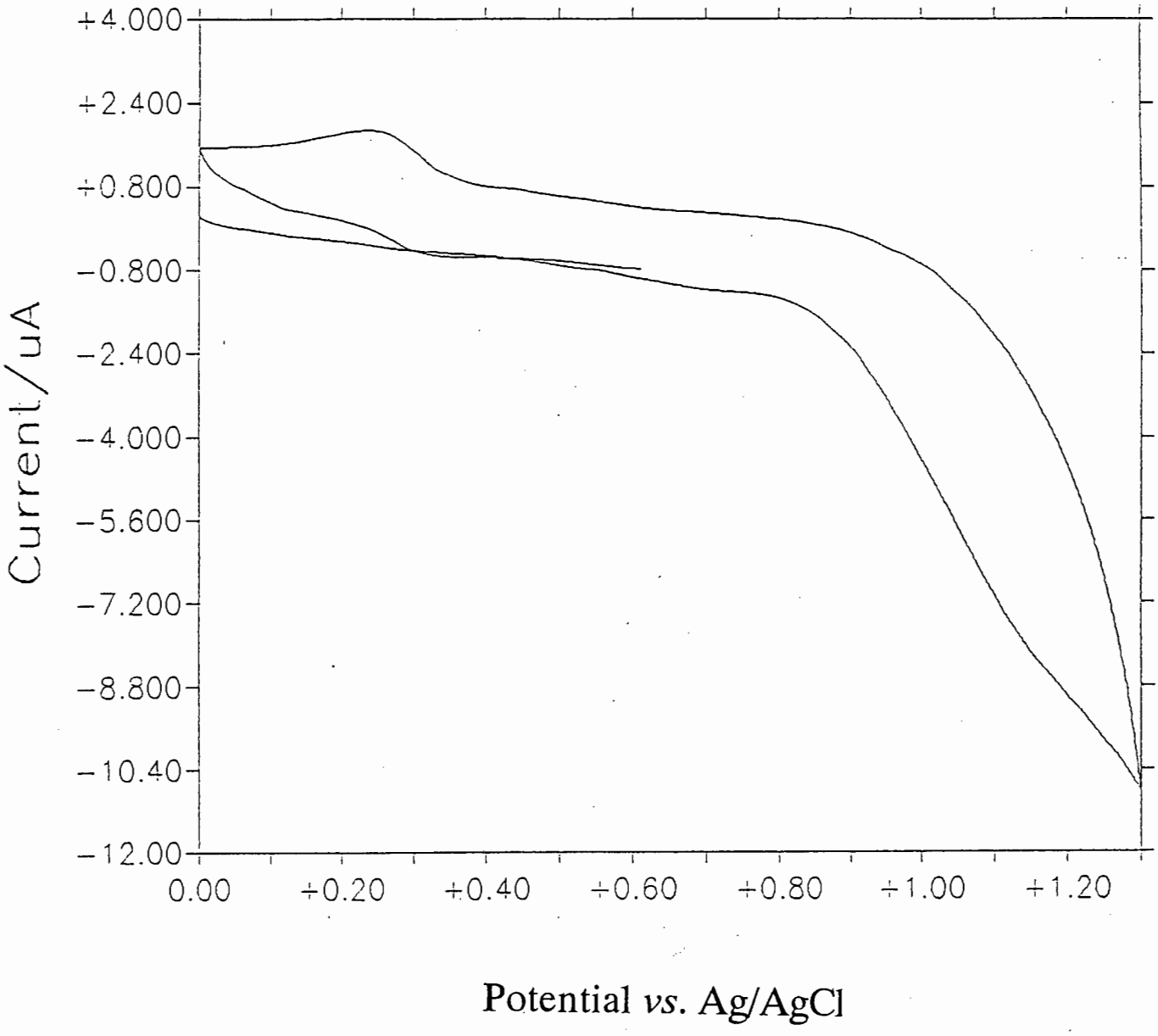

Figure 2.14 Cyclic voltammogram of 1.5×10^{-4} M $Fp(CH_2)_4Mp$ in 25 % acetonitrile in dichloromethane/0.1M $TBABF_4$.

These results firstly indicate the important role the solvent has to play in the mechanism following electrochemical activation of $Mp(CH_2)_nFp$. A strongly coordinating solvent such as acetonitrile may coordinate to the metal centre, should a vacant site become available. As a result, one may anticipate a chemical reaction to follow the oxidative electrode reaction of $Mp(CH_2)_nFp$ in the presence of acetonitrile.

Secondly, a comparison of the CV's of Fp-R and those obtained for $Fp(CH_2)_nMp$ (see Figures 2.10 to 2.13) suggest to us that:

(i) the electrochemical oxidation of $Mp(CH_2)_nFp$ in MeCN takes place as the successive oxidation of the two metal centres;

(ii) the first anodic wave represents the oxidation of the Fe side of the molecule and the second represents the oxidation of the Mo side. Thus both metals appear to behave independently of each other in these systems.

Earlier work by others[91-95] have shown that the electrochemical activity of Fp-R in MeCN shows an ECE mechanism whereas in CH_2Cl_2 an EC mechanism is followed. Carbonyl insertion and solvent incorporation take place in Fp-CH_3 systems after the initial irreversible one-electron oxidation. This $19e^-$ complex[94] is reduced on the reverse scan to render the neutral species as in Scheme 2-1.

In the oxidation of $Fp(CH_2)_nMp$, we view the successive abstraction of charge as being from either one or both metal centres in succession. Certainly an interesting feature of the irreversible anodic wave of these compounds (in acetonitrile) is the splitting thereof into two successive waves. If these two waves represent the abstraction of charge from the metal centres, then these centres should have different electron densities.

The oxidative properties of a few binuclear iron complexes (Table II-9) in dichloromethane were also investigated. Data were obtained from cyclic voltammograms in which scans were initiated from zero current potential in the positive direction up to 1.5 V (*vs* Ag/AgCl). These compounds were chosen since they contain metal centres of different electron environments due to the different ligands attached to them.

Table II-9 Oxidative properties of some homobinuclear iron compounds.

Compound	E_{ox} / V)[a]
$Fp(CH_2)_3Fp$	1.251
$Fp^*(CH_2)_3Fp$	1.005 and 1.196

[a] *Peak values, versus Ag/AgCl, $v = 100\ mV\ s^{-1}$*

The choice of dichloromethane as the solvent precludes the possibility of solvent participation in the mechanism that follows oxidation.

The absence of a delocalized π-system between the metal centres in these molecules impedes electronic interaction.[107-109] The difference in the potentials for the successive oxidations of the centres depends on the extent of the interaction between the sites.[107-109,114] In the complexes under study, one would expect the interaction to be minimal. In fact, the shape of the anodic wave for these complexes resembles that of a molecule containing a *single* electroactive centre. Hence it can be classified[114] as a species with non-interacting redox sites. Replacement of the one cyclopentadienyl ligand with a pentamethylcyclopentadienyl ligand results in a more electron-rich metal centre. Thus, the compound $Fp^*(CH_2)_3Fp$ contains two of the same metals but in different ligand environments. This difference is displayed in the two consecutive anodic waves found for this compound.

Cyclic voltammogram of $Fp(CH_2)_4Mp$ in MeCN including only the first oxidation wave thus resembles that of Fp-R (Figure 2.2). It is reasonable to suggest that the first anodic wave represents the oxidation at the Fe centre. The carbonyl insertion process can then occur at the Fe side of the molecule (Scheme 2-3). In contrast, it was found[118] that the chemical reaction of $Fp(CH_2)_nMp$

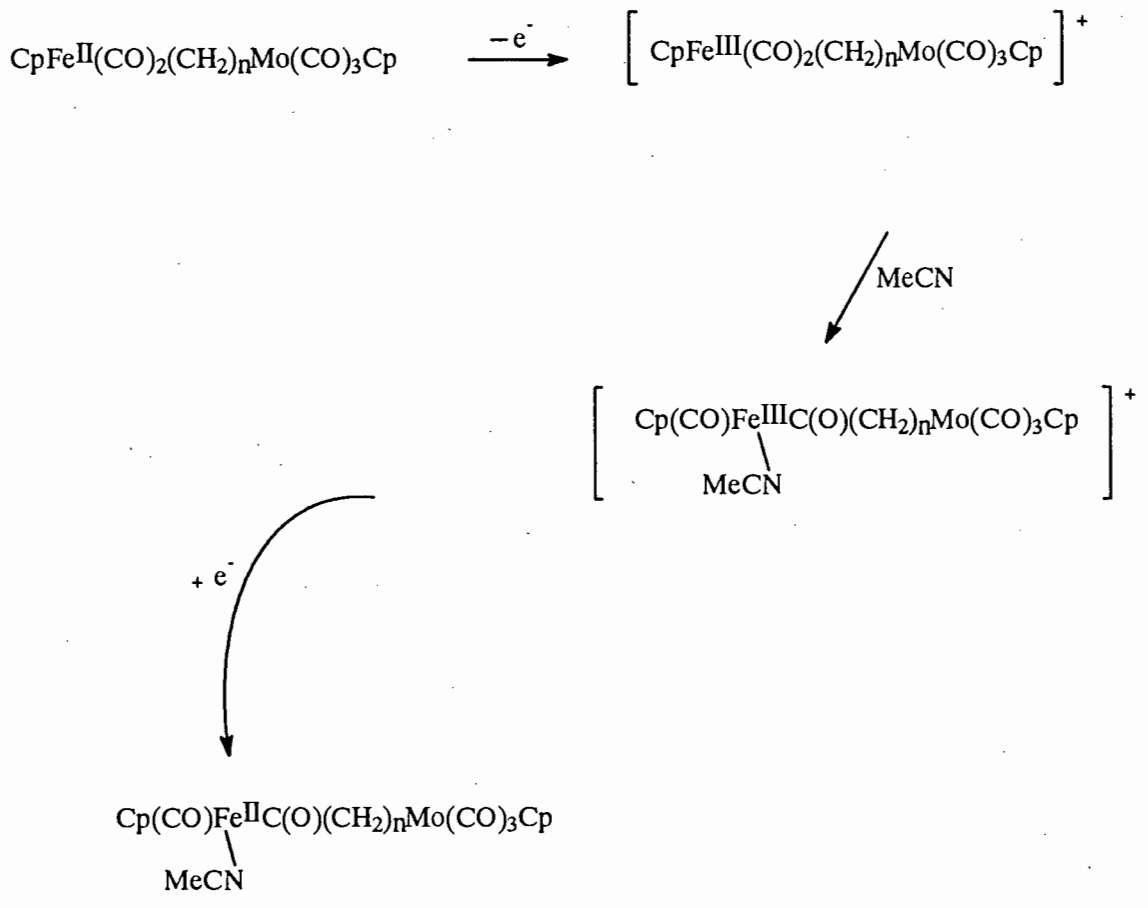

Scheme 2-3

(n = 3-6) with PPh_3 at room temperature (equation 2) was metalloselective with PPh_3 attack occurring at the Mo side of the molecule.

$$CpFe(CO)_2(CH_2)_nMo(CO)_3Cp \xrightarrow[CH_3CN]{PPh_3} CpFe(CO)_2(CH_2)_nC(O)Mo(PPh_3)(CO)_2Cp \quad ..(2)$$

Thus, the carbonyl insertion reaction takes place only at the Mo side in the presence of a strong nucleophile, and leaves the Fe side of the molecule intact.

Furthermore, the rates of CO insertion for the homodinuclear alkanediyl complexes of Mo were found to be greater than for the Fe analogues.

The infrared spectra of our heterobimetallic complexes in acetonitrile however, showed no presence of the acyl function. It is also known[991,92] that the rate of carbonyl insertion of Fp-R systems is enhanced by a factor of 10^6 upon one electron oxidation. This should be the overriding factor in support of our proposed mechanism.

Our results also imply that one can oxidize the Fe centre without oxidizing the Mo centre, and it requires less energy for the Fe centre to be activated electrochemically. The greatest ΔE value of 0.245 V was found for the complex $Cp(CO)_2Fe(CH_2)_6Mo(CO)_3Cp$. This small separation between the two successive anodic waves signifies a lack of a significant electronic interaction between the metal centres. This could be attributed to the absence of charge delocalization between the metals, the presence of which results in a separation of approximately 1 V between successive anodic waves.[107]

2.4 Conclusions

The electrochemical behaviour of the transitional metal alkyl complexes of the types $Cp(CO)_2Fe(CH_2)_nCH_3$ (n = 0 to 11), $Cp(CO)_3Mo(CH_2)_nCH_3$ (n = 2,3 and 16) and $Cp(CO)_2Fe(CH_2)_nMo(CO)_3Cp$ (n = 3 to 6) in acetonitrile and/or dichloromethane has been investigated. The behaviour of the iron alkyl compounds upon electrochemical oxidation was found to be solvent dependent. The oxidation potentials for the iron alkyl compounds as a function of the number of carbon atoms in the alkyl chain do not show any clear observable trends. The potentials can be correlated with the available Tolman's electronic parameters for the alkyl groups. The iron alkyl compounds yield, after initial electrochemical oxidation in acetonitrile, the corresponding acyl derivatives. The relative rates of decarbonylation for these acyl compounds was assessed using cyclic voltammetry, and the results agree satisfactorily with those obtained for other related systems. The oxidation potentials for the molybdenum alkyl complexes were found to be higher than for their corresponding iron alkyl analogues in acetonitrile. The reduction scans (obtained after the initial oxidation wave) for the molybdenum compounds show a number of small cathodic waves which we were unable to identify. The electrochemical behaviour of $Cp(CO)_2Fe(CH_2)_nCH_3$ and $Cp(CO)_2Mo(CH_2)_nCH_3$ proved to be very

useful in the interpretation of electrochemical data obtained for $Cp(CO)_2Fe(CH_2)_nMo(CO)_3Cp$.

The results for the oxidation of $Cp(CO)_2Fe(CH_2)_nMo(CO)_3Cp$ support the suggestion that the Fe centre of the molecule is oxidised first, followed by the oxidation of the Mo centre. Unambiguous assignment of the two successive anodic waves to the two metals, however might be achieved through the identification of the acyl species resulting from the CO insertion process occurring at the first anodic wave. This might be obtained using spectroelectrochemistry and investigating the infrared spectra in the $\upsilon(CO)$ region resulting from electrolysis at a slightly more anodic potential than the first oxidation peak. Other possible future work on the present systems could include cyclic voltammetric investigations at low temperature at which the alkyl migration reaction is slowed down. Kinetic measurements could be made by varying the scan rates. It would also be interesting to study the electrochemical behaviour (especially for the iron alkyl complexes) in more coordinating solvents e.g. dimethyl formamide or dimethyl sulphoxide. A strongly coordinating solvent molecule L, would act as a poor leaving group in the reaction

$$Cp(CO)FeC(O)(L)(R) \rightleftharpoons CpFe(CO)_2R + L,$$

greatly influencing the decarbonylation step. These conditions could also then be applied to the heterobimetallic systems.

Cyclic voltammetry has been shown to be a valuable tool for investigating the electrochemical behaviour of the complexes studied. This technique seems to offer much promise for significant and fascinating results of key importance in the field of mechanistic organometallic chemistry and should prove to be an area of vigorous future research endeavours.

CHAPTER 3

3.1 Experimental

Materials and synthesis of the complexes

The complexes $[CpFe(CO)_2(CH_2)_nMo(CO)_3Cp]$, n = 3 to 6, $[CpFe(CO)_2(CH_2)_3Fe(CO)_2Cp^*]$[118], $[CpFe(CO)_2(CH_2)_3Fe(CO)_2Cp]$[119] were synthesised according to literature procedures. All the iron alkyl complexes, $CpFe(CO)_2(CH_2)_nCH_3$, n = 0 to 11 were synthesised as previously described.[95] The molybdenum alkyl complexes $CpMo(CO)_3(CH_2)_nCH_3$, n = 2 and 16 were prepared according to the method described.[120]

Tetrahydrofuran (THF) was distilled over sodium before use. Acetonitrile and dichloromethane were distilled over P_2O_5 prior to use. Alumina (BDH, active neutral, Brockman grade 1) was deactivated before use. Tetrabutylammoniumtetrafluoroborate ($TBABF_4$) and ferrocene (both obtained from Sigma)were used as received and kept under vacuum.

Microanalyses were performed by the University of Cape Town Microanalytical Laboratory. Infrared spectra were recorded on a Perkin-Elmer 983 spectrometer. ^1H and ^{13}C NMR spectra were recorded on a Varian XR 200-MHz spectrometer. Tetramethylsilane (TMS) was used as an internal reference standard.

All organometallic complexes were judged pure from their infrared and ^1H NMR data prior to subjected to electrochemical measurements.

Synthesis and characterisation of $CpMo(CO)_3(CH_2)_3CH_3$

The dimer $[CpMo(CO)_3]_2$ (2.00g, 4.18 mmole) in THF (25 ml) was stirred over sodium amalgam (0.51g Na in 5 ml Hg) under N_2 for 1.5 hours at room

temperature. The resulting solution of $Na[CpMo(CO)_3]$ was transferred dropwise to a Schlenk tube containing n-butyl iodide (1.52g, 8.41 mmole) over 20 minutes. The reaction mixture was stirred for 15 hours at room temperature. After the solvent was removed the crude product was extracted with hexane (3 × 20 ml) and filtered. The filtrate was taken to dryness leaving a dark brown residue. This was transferred to an alumina column made up in hexane. Upon elution with hexane a yellow band was collected, concentrated and cooled to -78 °C. The product separated from this solution as yellow crystals. The mother liquor was syringed off and the product dried under reduced pressure. Yield: 1.50g (62%)

IR υ(CO) (hexane): 2018 cm^{-1} (vs) 1934 cm^{-1} (s). ^1H NMR ($CDCl_3$) δ 0.92 (t, 3H, CH_3), 1.35 (m, 2H, Mo-CH_2), 1.59 (m, 4H $CH_2CH_2CH_3$) ^{13}C NMR (TMS): δ 92.69 (Cp), 38.77 ($MoCH_2$), 28.39 (C_2), 13.67 (C_3), 2.37 (C_4)

Micro-analysis: Calculated for $C_{12}H_{14}O_3Mo$: C, 47.70; H, 4.68. Found: C, 47.26; H, 4.59

Electrochemical measurements

All electrochemical data were collected with the BAS CV 50W voltammograph connected to a printer. The three electrode cell used for cyclic voltammetry consisted out of a bright platinum disc (1.4 mm diameter) as the working electrode and a platinum wire electrode as the auxiliary electrode. A silver-silver chloride reference electrode was employed, separated from the sample compartment *via* a Luggin capillary, which was positioned as close as possible

(4 mm) to the working electrode. No *i*R compensation was used. Potentials were referenced relative to the ferrocenium/ferrocene (Fc^+/Fc) couple[121]. This was done by adding ferrocene to the sample solution after each experiment. The Fc^+/Fc couple was measured as 0.56 V *vs.* Ag/AgCl in CH_3CN and 0.46 V *vs.* Ag/AgCl in CH_2Cl_2, both solvents containing 0.1 M $TBABF_4$ as electrolyte. A scan rate of 100 mV s^{-1} was used unless otherwise stated. Potentials recorded were always reproducible to within 10 mV.

Solutions for cyclic voltammetry containing the organometallic complex had concentrations within the range of 0.2×10^{-3} M to 1.5×10^{-2} M. These solutions were purged with N_2 for 10 minutes prior to the experiment and kept under a N_2 blanket. After each scan both the working and auxiliary electrodes were repeatedly rinsed with distilled water and acetone and air dried. All experiments were performed at room temperature.

REFERENCES

1. W. E. Geiger, in *Laboratory Techniques in Electroanalytical Chemistry,* eds. P. T. Kissinger and W. R. Heineman, Marcel Dekker, New York, 1984, Chapter 18.

2. M. Chanon, *Acc. Chem. Res.*, **1987**, *20*, 214.

3. J. K. Kochi, *J. Organomet. Chem.*, **1986**, *300*, 139.

4. D. Astruc, *Angew. Chem., Int. Engl.*, **1988**, *27*, 643.

5. N. G. Conelly, *Chem. Soc. Rev.*, **1989**, *18*, 153.

6. J. A. Page and G. Wilkinson, *J. Am. Chem. Soc.*, **1952**, *74*, 6149.

7. T. Psarras and R. E. Dessy, *J. Am. Chem. Soc.*, **1966**, *88*, 5132.

8. R. E. Dessy, F. E. Stary, R. B. King and M. Waldrop, *J. Am. Chem. Soc.*, **1966**, *88*, 471.

9. R. E. Dessy, T. Chivers and W. Kitching, *J. Am. Chem. Soc.*, **1966**, *88*, 467.

10. R. E. Dessy, W. Kitching, T. Psarras, R. Salinger and A. Chen, T. Chivers, *J. Am. Chem. Soc.*, **1966**, *88*, 460.

11. R. E. Dessy, W. Kitching, T. Chivers and *J. Am. Chem. Soc.*, **1966**, *88*, 453.

12. R. E. Dessy, R. B. King and M. Waldrop, *J. Am. Chem. Soc.*, **1966**, *88*, 5112.

13. C. Jan and R. L. McCreery, *Anal. Chem.* **1986**, 58, 13, 2771.

14. R. M. Wightman and D. O. Wipf, *Acc. Chem. Res.* **1990**, *23*, 64 and references cited therein.

15. R. G. Compton and A. R. Hillman, *Chem. Br.*, **1986**, 1088.

16. A. J. Bard and L. R. Faulkner, *Electrochemical Methods, Fundamentals and Applications,* Wiley: New York, 1980: Chapter 11.

17. G. Heinze, *Angew. Chem. Int. Engl.*, **1984**, *23*, 11.

18. D. H. Evans, *Acc. Chem. Res.*, **1977**, *10*, 313.

19. G. A. Mabbott, *J. Chem. Educ.*, **1983**, *60*, 9.

20. D. H. Evans, *Chem. Rev.*, **1990**, *90*, 739.

21. J. K. Kochi, J. W. Hershberger and R. J. Klinger, *J. Am. Chem. Soc.*, **1982**, *104*, 3034.

22. K. M. Doysee, R. H. Grubbs and F. C. Anson, *J. Am. Chem. Soc.*, **1984**, *106*, 7819.

23. S. F. Nelsen, L. Echegoyen and D. H. Evans, *J. Am. Chem. Soc.*, **1973**, 97, 3530.

24. K. A. Rubinson, *Chemical Analysis*, Little Brown, Toronto. 1987: Chapter 12.

25. P. T. Kissinger and W. R. Heineman, *J. Chem. Ed.*, **1983**, *60*, 702.

26. K. A. Rubinson, *Chemical Analysis*, Little Brown, Toronto. 1987: page 422.

27. J. K. Kochi and R. J. Klinger, *J. Am. Chem. Soc.*, **1981**, *103*, 5839.

28. C. P. Andrieux, P. Hapiot and J. M. Saveant, *J. Phys. Chem.* **1988**, *92*, 5992.

29. D. O. Wipf and R. M. Wrightman, *Anal. Chem.* **1988**, *60*, 2460.

30. R. M. Wrightman and D. O. Wipf, *Acc. Chem. Res.* **1990**, *23*, 64.

31. J. Osteryoung, R. A. Osteryoung, R. Bilewicz and K. Wikiel, *Anal. Chem.*, **1989**, *61*, 965.

32. J. Osteryoung, R. A. Osteryoung and R. Bilewicz, *Anal. Chem.*, **1986**, *58*, 2761.

33. R. A. Osteryoung and J. Zeng, *Anal. Chem.*, **1986**, *58*, 2766.

34. R. L. McCreery and C. Jan, *Anal. Chem.*, **1986**, *58*, 2771.

35. T. Takanami, A. Abe, K. Suda and H. Ohmori, *J. Chem. Soc.,Chem. Commun.*, **1990**, 1310.

36. N. E. Murr, *J. Chem. Soc., Chem. Commun.*, **1981**, 251.

37. D. Pletcher and C. J. Pickett, *J. Chem. Soc., Dalton Trans.*, **1975**, *879*.

38. D. Pletcher and C. J. Pickett, *J. Chem. Soc., Chem. Commun.*, **1974**, *660*.

39. P. K. Baker, N. G. Conelly, B. M. R. Jones, J. P. Maher and K. R. Somers, *J. Chem. Soc., Dalton Trans.*, **1980**, *579*.

40. D. E. Walker, R. N. Adams and A L Juliard, *Anal. Chem.*, **1960**, *32*, 1526.

41. T. Kuwana, D. E. Bublitz and G. Hoh, *J. Am. Chem. Soc.*, **1960**, *82*, 5811.

42. I. V. Nelson and R. T. Iwamoto, *Anal. Chem.*, **1961**, *33*, 1795.

43. F. Farha and R. T. Iwamoto, *Anal. Chem.*, **1966**, *38*, 143.

44. H. M. Koepp, H. Wendt and H. Strehlow, *Z. Elektrochem.* **1960**, *64*, 483.

45. C. K. Mann and K. K. Barnes, *Electrochemical Reactions In Non-Aqueous Systems*, Marcel Dekker, Inc., New York. 1970; pp 419-425.

46. M. E. N. P. R. A. Silva, A. J. L. Pombeiro, J. J. R. Fraústo da Silva, R. Herrmann, N. Deus and R. E. Bozak, *J.Organomet. Chem.*, **1994**, *480*, 81.

47. M. Maggini, A. Karlsson, G. Scorrano, G. Sandonà, G. Farnia and M. Prato, *J. Chem. Soc., Chem. Commun.*, **1994**, 589.

48. B. Delavaux-Nicot, Y. Guari, B. Douziech, and R. Mathieu, *J. Chem. Soc., Chem. Commun.*, **1995**, 585.

49. C. K. Mann and K. K. Barnes, *Electrochemical Reactions In Non-Aqueous Systems*, Marcel Dekker, Inc., New York. 1970; p.201

50. J E Huheey, *Inorganic Chemistry; Principles of structure and reactivity*, Harper & Row Ed., 1978.

51. F. A. Cotton and G. W. Wilkinson, *"Advanced Inorganic Chemistry"*; 4th Ed., Wiley Interscience, New York, 1980; p 82.

52. Ref. 16, pp. 4-6.

53. A. C. Sarapu and R. F. Fenske, *Inorg. Chem.*, **1975**, *14*, 247.

54. Ref. 1, p 489.

55. J. Chatt, C. T. Kan, G. J. Leigh, C. J. Pickett and D. R. Stanley, *J. Chem. Soc., Dalton Trans.*, **1980**, 2032.

56. M. N. Golovin, M. M. Rahman, J. E. Belmonte and W. P. Giering, *Organometallics*, **1985**, *4*, 1981.

57. M. Rahman, H. Liu, A. Prock and W. P. Giering, *Organometallics*, **1987**, *6*, 650.

58. M. Rahman, H. Liu, K. Eriks, A. Prock and W. P. Giering, *Organometallics*, **1989**, *8*, 1.

59. A. Prock, W. P. Giering, J. E. Greene, R. E. Meirowitz, S. L. Hoffman, D. C. Woska, M. Wilson, R. Chang, J. Chen, R. H. Magnuson and K. Eriks, *Organometallics*, **1991**, *10*, 3479.

60. D. C. Woska, M. Wilson, J. Bartholomew, K. Eriks, A. Prock and W. P. Giering, *Organometallics*, **1992**, *11*, 3343.

61. D. C. Woska, J. Bartholomew, J. E. Greene, K. Eriks, A. Prock and W. P. Giering, *Organometallics*, **1993**, *12*, 304.

62. J. D. Atwood, M. J. Wovkulich and D. C. Sonnenberg, *Acc. Chem. Res.*, 1983, *16*, 350.

63. K. W. Barnett and T. G. Pollmann, *J. Organomet. Chem.*, 1974, *69*, 413.

64. K. Dahlinger, F. Falcone and A. J. Poë, *Inorg. Chem.*, 1986, *25*, 2654.

65. L. Chen and A. J. Poë, *Inorg. Chem.*, 1989, *28*, 2641.

66. C. A. Tolman, *Chem. Rev.*, 1977, *77*, 313.

67. Ref 51, p62.

68. T. Allman and R. G. Goël, *Can. J. Chem.*, 1982, *60*, 716.

69. G. M. Bancroft, L. Dignard-Bailey and R. J. Puddephatt, *Inorg. Chem.*, 1986, *25*, 3675.

70. F. Calderazzo, *Angew. Chem., Int. Ed. Engl.*, 1977, *16*, 299.

71. H. Berke and R. Hoffmann, *J. Am. Chem. Soc.*, 1978, *100*, 7224.

72. R.J. Mawby, F. Basolo and R.G. Pearson, *J. Am. Chem. Soc.*, 1964, *86*, 3994.

73. I.S. Butler, F. Basolo and R.G. Pearson, *Inorg. Chem.*, **1967**, *6*, 2074.

74. J.D. Cotton, G.T. Crisp and V.A. Daly, *Inorg. Chim. Acta*, **1981**, *47*, 165.

75. H. Brunner and B. Hammer, I. Bernal and M. Draux *Organometallics*, **1983**, *2*, 1595.

76. T.C. Forschner and A.R. Cutler, *Organometallics*, **1985**, *4*, 1247.

77. J.D. Cotton, G.T. Crisp and L. Latif, *Inorg. Chim. Acta*, **1981**, *47*, 171.

78. M.J. Wax and R.G. Bergman, *J. Am. Chem. Soc.* **1981**, *103*, 7028.

79. J.D. Cotton and R.D. Markwell, *Inorg. Chim Acta*, **1982**, *63*, 13.

80. S.J. LaCroce and A.R. Cutler, *J. Am. Chem. Soc.*, **1982**, *104*, 2312.

81. C.R. Jablonski and Y. Wang, *Inorg. Chim. Acta*, **1983**, *69*, 147.

82. T.C. Flood and K.D. Campbell, *J. Am. Chem. Soc.*, **1984**, *106*, 2853.

83. J.D. Cotton and R.D. Markwell, *Organometallics*, **1985**, *4*, 937.

84. S.L. Webb, C.M. Giandomenico and J. Halpern, *J. Am. Chem. Soc.*, **1986**, *108*, 345.

85. S. Levitre, A.R. Cutler and T.C. Forschner, *Organometallics*, **1989**, *8*, 1133.

86. J.D. Cotton and R.D. Markwell, *J. Organomet. Chem.*, **1990**, *388*, 123.

87. J.D. Cotton, M.M. Kroes, R.D. Markwell and E.A. Miles, *J. Organomet. Chem.*, **1990**, *388*, 133.

88. D. Monti and M. Basetti, *J. Am. Chem. Soc.* **1993**, *115*, 4658.

89. M. Bassetti, L. Mannina and D. Monti, *Organometallics*, **1994**, *13*, 3293.

90. M.F. Joseph, J.A. Page and M.C. Baird, *Inorg. Chim. Acta*, **1982**, *64*, L121.

91. R. H. Magnuson, S. Zulu, W. T'sai and W.P. Giering, *J. Am. Chem. Soc.*, **1980**, *102*, 6887.

92. R.H. Magnuson, R. Meirowitz, S. Zulu and W.P. Giering, *J. Am Chem. Soc.*, **1982**, *104*, 5790.

93. M.N. Golovin, R. Meirowitz, M. Rahman, H. Liu, A. Prock and W.P. Giering, *Organometallics*, **1987**, *6*, 2285.

94. W.C. Trogler and M.J. Therien, *J. Am. Chem. Soc.*, **1987**, *109*, 5127.

95. H. Liu, N.Golovin, D.A. Fertal, A.A Tracey, K. Eriks, W.P. Giering and A. Prock, *Organometallics*, **1989**, *8*, 1454.

96. A. Emeran, M. A. Gafoor, J. K. I. Goslett, Y. Liao, L. Pimble and J. R. Moss, *J. Organomet. Chem.* **1991**, *405*, 237 and references therein.

97. J. P. Bullock, M. C. Palazotto and K. R. Mann, *Inorg. Chem.*, **1991**, *30*, 1284.

98. A. J. Hart-Davis and R. J. Mawby, *J. Chem. Soc. (A)*, **1969**, 2403.

99. J. D. Cotton, G. T. Crisp and V. A. Daly, *Inorg. Chim. Acta*, **1981**, *47*, 165.

100. J. D. Cotton, H. A. Kimlin and R. D. Markwell, *J. Organomet. Chem.*, **1982**, *232*, C75.

101. J. D. Cotton and P. R. Dunstan, *Inorg. Chim. Acta*, **1984**, *88*, 223.

102. D. Astruc, *Acc. Chem. Res.*, **1986**, *19*, 377.

103. R. Q. Bligh, R. Moulton, A. J. Bard, A. Piórko, and R. G. Sutherland, *Inorg. Chem.*, **1989**, *28*, 2652.

104. W. J Bowyer, W. E. Geiger, and V. Boekelheide, *Organometallics*, **1984**, *3*, 1079.

105. W. H. Morrison, E. Y. Ho, and D. N. Morrison, *J. Am. Chem. Soc.*, **1974**, *96*, 3603.

106. W. H. Morrison, E. Y. Ho, and D. N. Morrison, *Inorg. Chem.*, **1975**, *14*, 500.

107. J. Kreisz, R. U. Kirss, and W. M. Reiff, *Inorg. Chem.*, **1994**, *33*, 1562.

108. L. O. Spreer, A. Li, D. B. MacQueen, C. B. Allan, J. W. Otvos, M. Calvin, R. B. Frankel, and G. C. Papaefthymiou, *Inorg. Chem.*, **1994**, *33*, 1753.

109. H. Wadepohl, C. von der Lieth, F. Paffen and H. Pritzkow, *Chem. Ber.*, **1995**, *128*, 317.

110. J. R. Hamon, D. Astruc and P. Michand, *J. Am. Chem. Soc.*, **1981**, *103*, 758.

111. M. V. Rajasekharan, S. Giezynski, J. H. Ammeter, N. Oswald, P. Michaud, J. R. Hamon, and D. Astruc, *J. Am. Chem. Soc.*, **1982**, *104*, 2400.

112. D. W. Clark, and K. D. Warren, *J. Organomet. Chem.*, **1978**, *152*, C60.

113. J. B. Flanagan, S. Margel, A. J. Bard, and F. C. Anson, *J. Am. Chem. Soc.* **1978**, *100*, 4248.

114. R. D. Taylor, J. P. Street, M. Minelli, and J. T. Spence, *Inorg. Chem.*, **1978**, *17*, 3207

115. C. Amiens, G. Balavoine, and F. Guibé, *J. Organomet. Chem.*, **1993**, *433*, 207.

116. J. M. Andersen and J. R. Moss, *Organometallics*, **1994**, *13*, 5013.

117. H. B. Friedrich and J. R. Moss, *J. Chem. Soc. Dalton Trans.*, **1993**, 2863.

118. H. B. Friedrich, J. R. Moss and B. K. Williamson, *J. Organomet. Chem.*, **1990**, *394*, 313.

119. R. B. King, *Inorg. Chem.*, **1963**, *85*, 531.

120. J. R. Moss and J. M. Andersen, unpublished results.

121. R. R. Gagné, C. A. Koval, G. C. Lisensky, Inorg. Chem., **1980**, *19*, 2854.